



UPPSALA  
UNIVERSITET

*Digital Comprehensive Summaries of Uppsala Dissertations  
from the Faculty of Medicine 1395*

# Preclinical PET imaging of Alzheimer's disease progression

XIAOTIAN T. FANG



ACTA  
UNIVERSITATIS  
UPSALIENSIS  
UPPSALA  
2017

ISSN 1651-6206  
ISBN 978-91-513-0151-8  
urn:nbn:se:uu:diva-333220

Dissertation presented at Uppsala University to be publicly examined in Rudbecksalen, Dag Hammarskjölds väg 20, Uppsala, Friday, 19 January 2018 at 09:15 for the degree of Doctor of Philosophy (Faculty of Pharmacy). The examination will be conducted in English. Faculty examiner: Professor Merja Haaparanta-Solin (University of Turku, Turku PET Centre, MediCity/PET Preclinical Laboratory, Finland).

### Abstract

Fang, X. T. 2017. Preclinical PET imaging of Alzheimer's disease progression. *Digital Comprehensive Summaries of Uppsala Dissertations from the Faculty of Medicine* 1395. 59 pp. Uppsala: Acta Universitatis Upsaliensis. ISBN 978-91-513-0151-8.

Amyloid PET imaging with [<sup>11</sup>C]PIB enabled detection of A $\beta$  for the first time *in vivo*. However, [<sup>11</sup>C]PIB is a small molecule that binds only the insoluble A $\beta$  plaque. Rather, the soluble A $\beta$  aggregates are considered the cause of Alzheimer's disease (AD). As such, a more sensitive and specific PET tracer is needed for tracking longitudinal AD pathology.

Soluble A $\beta$  aggregates likely interact with the metabotropic glutamate receptor 5 (mGluR5) to cause neurotoxic effects. However, with [<sup>11</sup>C]ABP688 PET we were unable to detect aberrant mGluR5 binding in AD mouse models, although we find elevated mGluR5 protein levels with immunoblotting.

Antibodies are highly specific large molecules that can bind specifically to soluble A $\beta$  aggregates, thus they can be a good marker for AD pathology. Unfortunately, due to their large size they cannot cross the blood-brain barrier (BBB). However, it is possible to shuttle antibodies into the brain by taking advantage of endogenous transporter systems on the BBB. By creating bispecific antibodies binding both to soluble A $\beta$  aggregates and to the transferrin receptor (BBB target), we successfully transported the antibody into the brain and could visually detect soluble A $\beta$  aggregates with PET.

Recombinant expression further improved and optimized antibody design, creating smaller bispecific antibody-based constructs that had better pharmacokinetic properties allowing for earlier PET scanning (1 day instead of 3), and more sensitive signal.

Lastly, using TCO-tetrazine click chemistry, we indirectly labeled our antibodies with fluorine-18, and could successfully perform PET already 11 h post-injection with a fluorine-18 labeled antibody.

*Keywords:* Alzheimer's disease, transgenic mice, PET, antibody-based tracer, mGluR5, ABP688, di-scFv, amyloid- $\beta$

*Xiaotian T. Fang, Department of Public Health and Caring Sciences, Box 564, Uppsala University, SE-75122 Uppsala, Sweden.*

© Xiaotian T. Fang 2017

ISSN 1651-6206

ISBN 978-91-513-0151-8

urn:nbn:se:uu:diva-333220 (<http://urn.kb.se/resolve?urn=urn:nbn:se:uu:diva-333220>)

Supervisors:

**Stina Syvänen, PhD**

Department of Public Health and Caring Sciences, Molecular Geriatrics, Uppsala University, Sweden

**Dag Sehlin, PhD**

Department of Public Health and Caring Sciences, Molecular Geriatrics, Uppsala University, Sweden

**Lars Lannfelt, MD, PhD, Professor**

Department of Public Health and Caring Sciences, Molecular Geriatrics, Uppsala University, Sweden

Faculty opponent:

**Merja Haaparanta-Solin, PhD, Professor**  
Turku PET Center, Faculty of Medicine,  
University of Turku, Finland

Examining committee:

**Anna Orlova, PhD, Professor**

Department of Medicinal Chemistry, Division of Molecular Imaging, Uppsala University, Sweden

**Markus Friden, PhD**

AstraZeneca and Department of Pharmaceutical Biosciences, Research; Division of Translational PKPD, Uppsala University, Sweden

**Per Nilsson, PhD**

Department of Neurobiology, Care Sciences and Society, Division of Neurogeriatrics, Karolinska Institutet, Sweden

Chairman:

**Marika Nestor, PhD**

Institute for Immunology, Genetics and Pathology, Medical Radiation Science, Uppsala University, Sweden



# List of papers

This thesis is based on the following papers, which are referred to in the text by their Roman numerals.

- I **Fang X.T.**, Eriksson J., Antoni G., Yngve U., Cato L., Lannfelt L., Sehlin D., Syvänen S. (2017) Brain mGluR5 in mice with amyloid beta pathology studied with in vivo [<sup>11</sup>C]ABP688 PET imaging and ex vivo immunoblotting. *Neuropharmacology*, 113: 293–300.
- II Sehlin, D., **Fang X.T.**, Cato L., Antoni G., Lannfelt L., Syvänen S. (2016) Antibody-based PET imaging of amyloid beta in mouse models of Alzheimer’s disease. *Nat Commun*, 7: 10759.
- III **Fang X.T.**, Sehlin D., Lannfelt L., Syvänen S., Hultqvist G. (2017) Efficient and inexpensive transient expression of multivalent antibodies in expi293 cells. *Biol Proced Online*, 19:11.
- IV **Fang X.T.**, Hultqvist G., Meier S.R., Antoni G., Sehlin D., Syvänen S. High detection sensitivity with antibody-based PET radioligand for amyloid beta in brain. *Submitted*.
- V **Fang X.T.**, Eriksson J., Olberg D.E., Gustavsson T., Antoni G., Lannfelt L., Sehlin D., Syvänen S. Fluorine-18 labeling of antibody-based PET constructs for amyloid beta. *Manuscript*.

Reprints were made with permission from the respective publishers.

# List of non-thesis publications

The following papers were published during the PhD period, but are not part of the thesis.

- I Hultqvist G., Syvänen S., **Fang X.T.**, Lannfelt L., Sehlin D. (2017) Bivalent Brain Shuttle Increases Antibody Uptake by Monovalent Binding to the Transferrin Receptor. *Theranostics*, 7: 308–318.
- II Syvänen S., **Fang X.T.**, Hultqvist G., Meier S.R., Lannfelt L., Sehlin D. (2017) A bispecific Tribody PET radioligand for visualization of amyloid-beta protofibrils – a new concept for neuroimaging. *Neuroimage*, 148: 55–63
- III Olsen M., Aguilar X., Sehlin D., **Fang X.T.**, Antoni G., Erlandsson A., Syvänen S. Astroglial responses to amyloid-beta pathology progression in a mouse model of Alzheimer’s disease. *Molecular Imaging and Biology*, in press
- IV Sehlin D., **Fang X.T.**, Meier S.R., Jansson M., Lannfelt L., Syvänen S. Pharmacokinetics, biodistribution and brain retention of a bispecific antibody-based PET radioligand for imaging of amyloid- $\beta$ . *Scientific Reports*, in press
- V Meier S.R., Syvänen S., Hultqvist G., **Fang X.T.**, Roshanbin S., Lannfelt L., Neumann U., Sehlin D. Antibody-based PET imaging detects lowered brain amyloid-beta levels after BACE-1 inhibition.” *Submitted*.

# Contents

Introduction	11
History of Alzheimer's disease	11
Amyloid $\beta$ protein precursor	12
Amyloid beta	12
Amyloid cascade hypothesis	14
Tau	15
CSF biomarkers	16
PET in AD	17
Metabotropic glutamate receptor 5	18
Immunotherapy	18
Antibodies	19
Blood-brain barrier	20
Receptor Mediated Transcytosis	21
Methodology	23
Animal models	23
In vivo imaging – positron emission tomography	24
PET data analysis	25
Antibody conjugation	27
Recombinant antibody expression	27
<i>Ex vivo</i> studies	28
Iodine-124 and iodine-125 labeling	29
Fluorine-18 labeling	29
SDS-PAGE and immunoblotting	30
Immunofluorescence	31
Cy3-labeling of antibodies	31
Enzyme linked immunosorbent assay	32
Aim	33
Results	35
Paper I	35
Paper II	36
Paper III	38
Paper IV	39
Paper V	39

Reflections	41
Concluding remarks	43
Acknowledgements	45
Summary	47
Samenvatting	49
References	51

# Abbreviations

$^{11}\text{C}$	Carbon-11
$^{18}\text{F}$	Fluorine-18
$^{124}\text{I}$	Iodine-124
$^{125}\text{I}$	Iodine-125
1TCM	One-tissue compartment model
A $\beta$	Amyloid beta
A $\beta$ PP	Amyloid beta precursor protein
AD	Alzheimer's disease
BBB	Blood-brain barrier
BP <sub>nd</sub>	Nondisplaceable binding potential
C <sub>img</sub>	Image derived radioactivity concentration
CSF	Cerebrospinal fluid
CT	Computed tomography
di-scFv	Di-single-chain variable fragment
ELISA	Enzyme-linked immunosorbent assay
EOAD	Early onset Alzheimer's disease
FDG	Fludeoxyglucose
FMRP	Fragile X mental retardation protein
FXS	Fragile X syndrome
GFAP	Glial fibrillary acidic protein
HRP	Horseradish peroxidase
<i>ID/BW</i>	Injected dose per bodyweight
IgG	Immunoglobulin G
K <sub>p</sub>	Brain-to-blood ratio
KPI	Kunitz protease inhibitor
LTD	Long-term depression
LTP	Long-term potentiation
MCI	Mild cognitive impairment
mGluR5	Metabotropic glutamate receptor 5
MRI	Magnetic resonance imaging
NFT	Neurofibrillary tangle
PAGE	Polyacrylamide gel electrophoresis

PBS	Phosphate buffered saline
PET	Positron emission tomography
PIB	Pittsburgh compound B
PrP <sup>c</sup>	Cellular prion protein
<i>PSEN1</i>	Presenilin-1
<i>PSEN2</i>	Presenilin-2
P-tau	Phosphorylated tau
PVDF	Polyvinylidene fluoride
RMT	Receptor-mediated transcytosis
ROI	Region of interest
scFv	Single-chain variable fragment
sdAb	Single-domain antibody
SDS	Sodium dodecyl sulfate
SNR	Signal-to-noise ratio
SRTM	Simplified reference tissue model
SUV	Standardized uptake value
SUVR	Standardized uptake value ratio
TCO	Tetra cyclooctene
TfR	Transferrin receptor
TMB	3,3',5,5'-Tetramethylbenzidine
T-tau	Total tau
V <sub>T</sub>	Total distribution volume

# Introduction

Current clinical diagnosing of Alzheimer's disease (AD) relies on neuropsychological testing, behavioral testing, and the experiences of relatives; though only *post mortem* histology provides definitive disease confirmation. Furthermore, tests for cognitive decline reveal AD when already the neuropathology has been underway for years prior to the manifestation of cognitive symptoms. Considering there is no cure for AD, prevention has garnered much attention, which has led to increased interest for *in vivo* imaging of the molecular changes causing AD.

One major breakthrough was the development of Pittsburgh compound B (PIB), enabling for the first time *in vivo* visualization of AD pathology. [<sup>11</sup>C]PIB is a small molecule, radioactively labeled with carbon-11 (<sup>11</sup>C), which binds amyloid beta (A $\beta$ ) plaques in the brain [1]. However, this radioligand is not an ideal biomarker, since the signal changes little with disease progression [2–4]. Moreover, amyloid deposition can be identified (with PIB PET) among cognitively normal elderly persons during life, and have amyloid deposition in the brain as confirmed *post mortem* [2, 5]. This suggests that an elderly person with significant amyloid burden can remain cognitively normal, however these persons are more likely to develop AD eventually [6].

As such, there is a need for a biomarker capable of visualizing the dynamic changes in pathophysiology causing or underlying AD from an early stage of the disease progress.

## History of Alzheimer's disease

Alzheimer's disease is the most common form of dementia. It was first described by Alois Alzheimer in 1906, when he characterized the histological changes found in the brain of his patient, Auguste D, who had dementia [7]. AD is a degenerative disease of the brain. Clinically, this manifests as progressively worse cognitive functioning ultimately leading to death. Auguste D started showing symptoms now associated with dementia, such as memory loss, delusions, frequent mood changes, she forgot details about her life and gave incoherent answers when questioned. The peculiarity of her case was that her clinical symptoms appeared at a much earlier age than typical of other patients with a degeneration of the psyche, as Auguste D was likely in her early forties, and usually AD occurs in their seventies.

More than a century later, a genetic reexamination of her histological brain tissue led to the finding of a mutation in presenilin-1 (*PSEN1*), which leads to an early onset inheritable form of AD [8]. The two characteristic changes that Alzheimer found in her brain during *post mortem* histological examination were large plaque shapes containing A $\beta$ , and intracellular neurofibrillary tangles (NFT) composed of tau protein. Likely as a result of these protein aggregates, the third hallmark of AD occurs: atrophy of the brain.

## Amyloid $\beta$ protein precursor

The actual cause of AD has remained largely unknown. A $\beta$  has been the major focus of study, and the A $\beta$  plaques were at first considered toxic and the reason for the disease. The A $\beta$  peptide is produced by two enzymatic cleavages of the amyloid  $\beta$  protein precursor (A $\beta$ PP) [9]. The highly conserved gene encoding for A $\beta$ PP in humans is located on chromosome 21, with three major *A $\beta$ PP* mRNA splice variants: A $\beta$ PP<sub>751</sub>, A $\beta$ PP<sub>770</sub>, and A $\beta$ PP<sub>695</sub> (lacking the Kunitz protease inhibitor (KPI) subdomain, which is present in the other two) [10–12]. *A $\beta$ PP* mRNA is expressed in cortical and hippocampal region neurons and the distribution is similar to that of NFTs in AD but *A $\beta$ PP* mRNA was found to be present in neurons usually not involved in AD pathology as well [13]. It is a cell surface protein, and its crystal structure reveals an extracellular domain containing a growth factor-like and a copper-binding domain [14]. Evidently, one theory of AD etiology is a deregulated homeostasis of metal ions [15]. This alludes to possible dysfunctioning of A $\beta$ PP as a cause for AD. The A $\beta$  peptide is produced when A $\beta$ PP is first proteolytically cleaved by  $\beta$ -secretase followed by another cleavage by  $\gamma$ -secretase (which has multiple possible cleavage sites), releasing a peptide that varies in length between 36–43 amino acids (i.e. the amyloidogenic pathway, **Figure 1**) [16]. The most common variants are the 40 amino acid long peptide (A $\beta$ 40) and the 42 amino acid long (A $\beta$ 42).

## Amyloid beta

The plaques first reported by Alois Alzheimer were found to contain A $\beta$  by Wong and colleagues in 1985, and it was then first suggested that the pathogenesis of AD involves A $\beta$ . Other clues include that people with trisomy 21 exhibit signs of AD before the age of 50, due to increased A $\beta$  production from the extra chromosome 21 which has the *A $\beta$ PP* gene [17, 18]. Indeed, there is a small subpopulation of AD patients (<5%), also known as early onset AD (EOAD), that present clinical signs of AD before the age of 65. Early onset forms of AD are characterized by having a mutation in genes coding for either *A $\beta$ PP*, *PSEN1* or presenilin-2 (*PSEN2*).

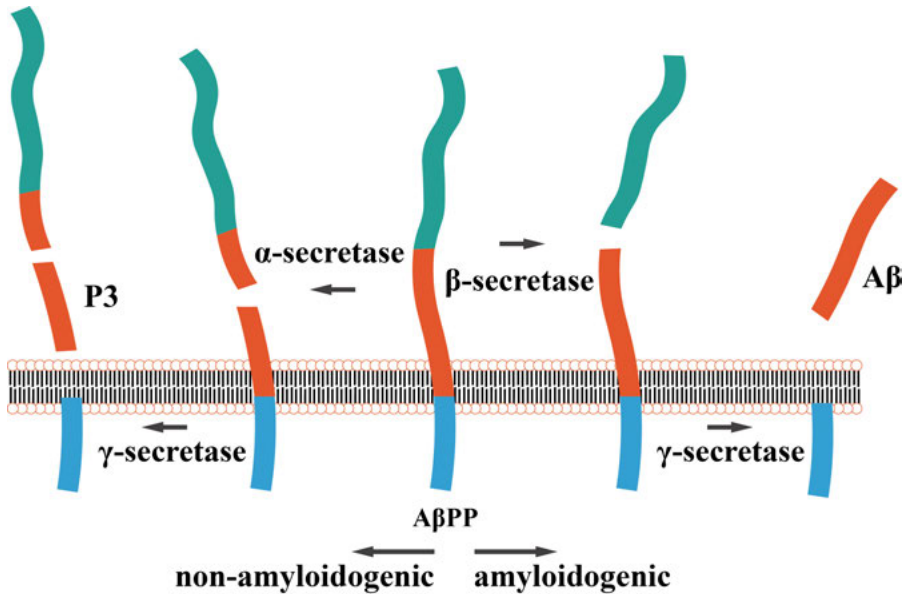


*Figure 1.* Schematic visualization of A $\beta$ PP cleavage. The A $\beta$  amino acid sequence is partly embedded in the transmembrane domain (TMD). There are two pathways, the non-amyloidogenic (initiated when cleavage in the A $\beta$  sequence occurs by  $\alpha$ -secretase, followed by  $\gamma$ -secretase, creating p3) and the amyloidogenic pathway which produces A $\beta$ . For full length A $\beta$  to be formed, first proteolytic cleavage by  $\beta$ -secretase has to occur, followed by a cleavage by  $\gamma$ -secretase, leading to the release of A $\beta$ .

Unlike the cases of late onset AD, early onset cases can be explained solely by mutations in one of these genes [19]. These mutations are found to be familial and are passed on in an autosomal dominant manner. The mutations in *A $\beta$ PP* lead to AD pathology by affecting A $\beta$  in some way, i.e. carriers of the Swedish mutation (KM670/671NL) have increased production and secretion of A $\beta$ , and higher levels of total A $\beta$  [20]. The Arctic mutation (E693G) increases the tendency of A $\beta$  to favor formation of protofibrils (i.e. large oligomers), and plasma levels of A $\beta$ 40 and A $\beta$ 42 are lower in Arctic mutation carriers [21, 22]. On the other hand, the Icelandic mutation (A673T) is protective against AD. This polymorphism leads to 40% lower A $\beta$  formation *in vitro* [23, 24]. Disease-linked mutations in *PSEN1* and *PSEN2* have also been found [25]. Presenilin-1 and 2 are subunits of the  $\gamma$ -secretase complex, which cleaves A $\beta$ PP to form A $\beta$ . Mutations in catalytic enzymes involved in A $\beta$  production lead to AD pathology, if these mutations have deregulatory effects causing overproduction of A $\beta$ 42 or change the A $\beta$ 40/42 ratio [26–31]. It is evident now that A $\beta$  has a role in AD disease pathology.

## Amyloid cascade hypothesis

First proposed by John Hardy and Gerald Higgins in 1992, the amyloid cascade hypothesis is that the deposition of A $\beta$  protein, the major component of amyloid plaques, is the causative event of AD pathology [32]. Neurofibrillary tangles, cell loss, vascular damage, and dementia follow as a direct result of this deposition [32]. As such, amyloid pathology (at the time thought to be plaques) is the first event and is the direct cause of AD. These plaques are the final step in a (possibly reversible) pathway starting with monomeric A $\beta$  (**Figure 2**).

First, monomers undergo a conformational change, which induces aggregation into dimers, trimers, tetramers, and/or other larger aggregates of various sizes. These intermediary arrangements are known as oligomers and on the larger end of the scale as protofibrils. These forms of A $\beta$  are soluble, while the large plaques made out of fibrils are insoluble, and as such they are deposited into plaque structures. Further supported by the discoveries that familial forms of AD are caused by mutations that lead to increased production of A $\beta$ , and based on the amyloid cascade hypothesis, current therapeutic intervention strategies have often been focused on the ‘A $\beta$ -economy’, i.e. reducing A $\beta$  production, facilitating A $\beta$  clearance, and preventing A $\beta$  aggregation [33].

A $\beta$  plaques are a key histological sign of AD, but they correlate poorly with severity of dementia, rather it is the loss of synapse that correlates best with the level of cognitive impairment [34]. Instead, it is the intermediary soluble A $\beta$  species (i.e. oligomers and protofibrils) that may be the disease causing forms of A $\beta$ . Soluble A $\beta$  concentrations correlate better with synaptic loss and possibly due to their solubility, they have more potential of affecting neurons and glial cells [35–42]. It is suspected that especially the higher order oligomer/protofibrillar forms of A $\beta$  may be the most neurotoxic [39, 43–46].

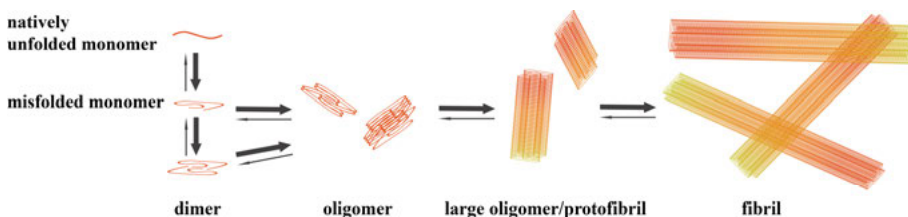


*Figure 2.* A $\beta$  aggregation pathway. Protein misfolding causes aggregation of monomeric A $\beta$  into dimeric assemblies, which aggregate further into larger accumulations (e.g. tetramers) and into oligomers, which are heterogeneous and span a wide molecular range. Oligomers form larger aggregates (i.e. higher order oligomers and protofibrils), until they ultimately form insoluble fibrils that make up the amyloid plaques. Of the soluble species, it is thought that the oligomers and protofibrils are most likely the toxic species responsible for pathology.

In a study performed to clarify the role of soluble A $\beta$  aggregates (i.e. oligomers and protofibrils), two different mouse lines overexpressing A $\beta$ PP were compared; the A $\beta$ PP23 and the A $\beta$ PP51/16 mouse lines. The A $\beta$ PP23 mouse overexpresses A $\beta$ PP with the Swedish mutation, while the A $\beta$ PP51/16 overexpresses wild type human A $\beta$ PP. Both mouse lines develop A $\beta$  plaques, but the A $\beta$ PP23 mouse exhibited higher levels of soluble A $\beta$  oligomers, protofibrils, and fibrils. Furthermore, only the A $\beta$ PP23 mouse showed signs of pathology in the forms of neuronal degeneration, neuron loss, and loss of asymmetric synapses [47].

Evidently it appears that A $\beta$  oligomers are involved in disease pathology. Naturally secreted A $\beta$  oligomers inhibit hippocampal long-term potentiation (LTP) *in vivo* in rats, and A $\beta$  oligomers levels correlate to spatial learning deficits [37, 48]. When pretreated with A $\beta$  monomer degrading enzymes, LTP was still hindered, indicating that it is the soluble oligomeric forms of A $\beta$  that possess neurotoxicity. When cells were treated with  $\gamma$ -secretase inhibitors, oligomer formation was lower and LTP was no longer hindered, demonstrating that therapeutic intervention of AD pathology may be a possibility [37].

## Tau

The second hallmark Alois Alzheimer reported were the ‘tangles’ of intracellular structures in the brain of Auguste D, however it wasn’t until the 1986 that it was discovered that these tangles consisted of tau protein [49]. Tau refers to microtubule-associated proteins (MAP) expressed from the *MAPT* gene found on chromosome 17 [50]. There are six major brain tau isoforms ranging between 352 and 441 amino acids in length as the result of alternative splicing of exons 2, 3, and 10 [51]. Tau proteins are expressed primarily in neurons, but are also found in glial cells [52].

One of the main functions of tau is to modulate and stabilize axonal microtubules. However, this role does not appear to be essential. Tau knockout mice (i.e. lacking tau protein expression) are viable and do not present with an overt phenotype, it is likely that the loss of tau expression can be compensated for by other MAPs [53].

Tau is natively unfolded and highly soluble, however it has a tendency to form a hairpin fold that is not permissive for aggregation [54–56]. Tau aggregation likely requires conformational changes in monomers as well as the formation of stable oligomeric complexes that can act as nucleation units [57]. Adding preformed amyloid tau assemblies *in vitro* accelerates the formation of tau amyloid fibrils by recruiting monomeric tau [58]. Furthermore, introducing misfolded preformed tau fibrils into tau-expressing cells rapidly recruits large amounts of soluble tau into filamentous inclusions resembling NFTs, which suggests a seeding process as the mechanism underlying NFT formation *in vivo* [59].

The aggregated tau found in AD brain consists of all six kinds of brain tau isoforms that are heavily phosphorylated at more than 40 different Ser and Thr residues [60, 61]. Furthermore, tau hyperphosphorylation precedes the formation of NFTs, and can be considered a prominent distinction between pathological tau and normal tau [62].

## CSF biomarkers

The cerebrospinal fluid (CSF) is the body fluid found both in the brain and in the spinal cord. It submerges the brain, acting as a physical cushion. There is approximately a total volume of 125 ml at any time, but about 500 ml is generated daily. It is produced in the choroid plexuses of the brain, and absorbed in the arachnoid granulations. The CSF is derived from blood plasma, and the main distinction is that CSF is nearly protein-free compared with plasma. CSF can be obtained and tested for diagnosis after obtaining it via lumbar puncture. The rationale behind testing the CSF for AD biomarkers is the fact that the CSF is in direct contact with the extracellular space of the brain. The interstitial fluid in the extracellular space is secreted into the CSF, and thus biochemical changes in the brain are likely to be reflected in CSF. The finding of A $\beta$  peptide in CSF further strengthens suitability of detecting biomarkers in CSF [63]. Initially, levels of total A $\beta$  were investigated and no differences between AD patients and controls could be found [64].

Instead, emphasis has shifted towards A $\beta$  isoforms, most notably A $\beta$ 42. In AD patients, a reduced level of A $\beta$ 42 in CSF was reported compared with healthy controls [65]. The reduction in A $\beta$ 42 level is likely caused by the aggregation and accumulation in the plaques, as CSF A $\beta$ 42 levels have been found to correlate with plaque load in the neocortex and hippocampus of AD patients [66, 67]. Thus, lowered levels of CSF A $\beta$ 42 is an accurate and widely used AD biomarker.

On the other hand, CSF A $\beta$ 40 does not appear to change in AD [68]. As such, the ratio of A $\beta$ 40/42 in CSF is increased in AD patients [69]. This change in ratio appears to have better diagnostic performance than only based on A $\beta$ 42 levels [70].

Both total tau (T-tau), and phosphorylated tau (P-tau) can be detected in the cerebrospinal fluid and are suitable biomarkers for AD [71]. T-tau levels in CSF probably reflect intensity of neuronal damage and degeneration, based on marked transient increases in CSF T-tau that correlate with CT-based measurements of infarct size in acute stroke [72]. Furthermore, the highest reported CSF T-tau levels were found in Creutzfeldt-Jakob disease patients, where intense neuronal degeneration occurs [73].

Phosphorylated forms of tau are also found in the CSF. The CSF levels of P-tau likely reflect the phosphorylation state of tau, as P-tau levels do not

change after acute stroke, although T-tau does [74]. As such, it is likely that P-tau is a potential biomarker for tangle formation in AD brain.

The diagnostic potential of combining CSF measurements for tau and A $\beta$  has also been investigated. Combinatorial diagnosis relying both CSF T-tau and A $\beta$ 42 has higher sensitivity and specificity than relying on T-tau or A $\beta$ 42 independently [71].

## PET in AD

The other most common diagnostic marker for AD now is amyloid PET. Currently one of the most commonly used PET ligands for visualizing A $\beta$  in the brain is [ $^{11}\text{C}$ ]PIB, which is a radioactively labeled derivative of thioflavin-T. The first *in vivo* PET studies were performed by Klunk et al. in 2004 and they successfully visualized A $\beta$  plaques in AD patients [1]. [ $^{11}\text{C}$ ]PIB binds to the  $\beta$ -sheet structure of amyloid fibrils that make up the A $\beta$  plaques, and in grey matter the binding of [ $^{11}\text{C}$ ]PIB to A $\beta$  is specific and reversible.

However in white matter [ $^{11}\text{C}$ ]PIB behaves differently, the white matter component has a non-specific and non-saturable component which may be due to the high lipid content in white matter, and possibly also due to the  $\beta$ -sheet structure present in myelin [75]. [ $^{11}\text{C}$ ]PIB PET allows for longitudinal evaluation of white matter, and can be used to quantify myelin loss and regeneration [76, 77]. While white matter uptake is much lower than in grey matter, the uptake is prominent at later time points due to slower kinetics in white matter. This leads to partial volume effects, and to an overestimation of [ $^{11}\text{C}$ ]PIB binding estimation in healthy subjects [78].

A common method to quantify amyloid load is to calculate the region-to-cerebellum ratio over 60-90 minutes [79]. Here it is assumed that any increase in ratio is due to the presence of specific binding, as the cerebellum is considered a region void of A $\beta$  pathology.

What is problematic with [ $^{11}\text{C}$ ]PIB is that the PET signal has been reported to remain static while pathology progresses [3, 4]. In a follow-up study to the original [ $^{11}\text{C}$ ]PIB study by Klunk et al, no significant difference in [ $^{11}\text{C}$ ]PIB retention was found between baseline and follow-up, while a significant 20% decrease in regional metabolic rate as assessed with fluorodeoxyglucose ( $^{18}\text{F}$ )FDG) PET could be observed [4]. [ $^{18}\text{F}$ ]FDG is a fluorine-18 labeled glucose analogue, and [ $^{18}\text{F}$ ]FDG uptake is a marker for glucose uptake, which is then subsequently a correlate of tissue metabolism. This could likely be due to the fact that A $\beta$  pathology is one of the earliest occurring events, and A $\beta$  plaque deposition has already reached a saturated level prior to later changes, e.g. NFTs, synaptic loss, lower metabolism [80].

[ $^{11}\text{C}$ ]PIB as a diagnostic marker appears to be highly sensitive and also specific. In pathologically confirmed cases of dementia [ $^{11}\text{C}$ ]PIB PET had a sensitivity of 100%, and a specificity of 88-92% for AD [81]. In cohorts of people

with mild cognitive impairment (MCI), [ $^{11}\text{C}$ ]PIB PET is estimated to have a sensitivity of 96%, but a much lower specificity of 58% based on a review of nine studies [82]. This implies that for every 100 [ $^{11}\text{C}$ ]PIB scans, one person with a negative scan would progress into AD, and 28 with a positive scan would not progress into AD, assuming a typical conversion rate of MCI to AD of 34%. As such, while [ $^{11}\text{C}$ ]PIB is highly suited for detecting and diagnosing AD, the predictive value and usage for longitudinal assessment of dynamic changes is perhaps lacking.

## Metabotropic glutamate receptor 5

The metabotropic glutamate receptor 5 (mGluR5) is a postsynaptically expressed G-protein coupled protein that plays a role in downstream signaling and  $\text{Ca}^{2+}$  regulation. It is involved in regulating LTP, and in learning and memory, and it is believed to be involved in mediating  $\text{A}\beta$  toxicity [83, 84]. Blocking of mGluR5 functioning with antagonists has been found to be neuroprotective in cortical cultures, indicating that mGluR5 is being involved in neurotoxic signaling. Furthermore, selectively blocking of mGlu5 receptors was also reported to be protective against  $\text{A}\beta$  toxicity [85]. Evidently, an interaction between mGluR5 and  $\text{A}\beta$  oligomers seems to exist, and mGluR5 may be a link between  $\text{A}\beta$  and pathology.

Recently, insights were gained into the mechanisms of interaction between  $\text{A}\beta$  oligomers and mGluR5.  $\text{A}\beta$  oligomers disrupt normal mGluR5 signaling by hindering their diffusional properties on the membrane, which leads to accumulation of mGluR5 at the synapses. As a result of this clustering, mGluR5 elevates intracellular calcium and causes synapse deterioration. Clustering of mGluR5 by artificial crosslinking leads to similar toxic effects [84].  $\text{A}\beta$  oligomers form a complex together with cellular prion protein ( $\text{PrP}^{\text{C}}$ ) and mGluR5, and facilitates long-term depression (LTD) as a result. The ability of  $\text{A}\beta$  oligomers to induce LTD appears to require the presence of mGluR5, and this process can be blocked with mGluR5 antagonists [83, 86]. Crossing the AD mouse model  $\text{A}\beta\text{PP}_{\text{Swe}}/\text{PS1}_{\Delta\text{E9}}$  with an mGluR5 knockout mouse line creates a resultant mouse with reduced cognitive impairment and pathogenesis [87]. Evidently, mGluR5 is strongly implied to be involved in early stage disease AD pathology and it plays a key role in mediating neurotoxicity in the presence of soluble  $\text{A}\beta$  aggregates. Therefore, it is an interesting candidate as a diagnostic marker for early pathological changes in AD.

## Immunotherapy

Immunotherapy is a promising emerging field of therapeutics based on eliciting or modulating an immune response to treat disease. The first treatment

approach was vaccination, i.e. active immunization with the A $\beta$ 42 peptide. Actively immunizing PDAPP transgenic mice (overexpresses human A $\beta$ PP with the Indiana mutation, V717F) with A $\beta$  peptide prevented A $\beta$  plaque formation and ameliorated cognitive deficits [88–90]. However a clinical trial with AN1792 (vaccine containing A $\beta$ 42 and QS21, a purified plant extract which enhances the immune response to antigens) found detrimental T-cell-mediated inflammatory responses, and cognitive benefits were modest compared with the placebo group, however this could be attributed in part to the small decline in cognition in the placebo group [91–93]. Furthermore, persistent late-stage tau-pathology in cortical regions cleared of amyloid may indicate that intervention was too late. A follow-up study of the AN1792 trial found significant A $\beta$  plaque clearance while there was no evidence of improved survival or longer time until severe dementia [94]. In transgenic mice (3xTg-AD) antibodies against A $\beta$  cleared early, but not late, forms of hyperphosphorylated tau aggregates [95].

Passive immunization with A $\beta$  specific antibodies administered peripherally have been shown to lower pathology and neuronal abnormalities in transgenic mouse brain [89, 96, 97]. A large majority of monoclonal antibodies as therapeutics have failed in clinical trials due to side effects, lack of clinical efficacy, but also due to misdiagnosing of the enrolled patients. A diagnosis based on clinical symptoms is difficult to make, and in the bapineuzumab (one of the most well studied antibodies against A $\beta$ ) trials approximately 30% of the enrolled AD group likely did not have the disease. As such, today's trials now have inclusion criteria, i.e. PET and/or CSF biomarkers [98]. A recent publication on aducanumab (which selectively targets aggregated A $\beta$ ) showed a dose dependent reduction in plaque burden in AD patients as measured with florbetapir PET (fluorine-18 analogue of PIB) accompanied by a slowing of clinical decline [99]. Currently, a humanized version (BAN2401) of the mAb158 antibody targeting A $\beta$  protofibrils is in clinical trial [100]. As such, it would seem that immunotherapy for AD still holds great promise.

## Antibodies

Antibodies, or immunoglobulins, are large proteins (conventionally sized at 160 kDa) endogenously produced by the plasma cells of the immune system as part of the inflammatory process for neutralizing foreign pathogens such as intruding bacteria and viruses. There are several classes of antibodies, but it is the IgG class (immunoglobulin G) that is the most common type, and also the main format involved in the immune response.

Conventional IgG antibodies are composed out of two heavy chains and two light chains. The tail of the antibody (i.e. Fc region) can bind Fc receptors and is the part that is involved in the immune response, the other part is the antigen binding domain (Fv region), which can recognize and bind a specific

target (i.e. peptide sequence, lipids, polysaccharides). Their unique property to bind any potential target being presented has led to their extensive application in research. Specific antibodies can be created by injecting an antigen (generally a peptide sequence or fragment of a target of interest) into a mammal, such as a mouse, rat, or rabbit. Blood isolated from these animals will contain polyclonal antibodies (i.e. antibodies from different B cell lineages binding to the same antigen) against the injected antigen. Monoclonal antibodies can be produced by isolating antibody-producing lymphocytes and fusing them with a cancer cell line, creating hybridomas, which will produce monoclonal antibodies.

By producing antibodies recombinantly, it is possible to perform protein engineering, i.e. modifying and customizing antibodies in many different ways. This is done by first determining the protein structure of an antibody, most commonly by X-ray crystallography or computational modeling. Once the protein sequence is known, it can be reverse translated into a nucleotide sequence encoding the antibody. This can be incorporated into a DNA plasmid and by then transfecting a cell line with the sequence, it will produce recombinant antibody. Another advantage is that the sequence can be modified, i.e. with a recombinant approach it is possible to design protein structures based on antibodies. For example, it is possible to create an antibody-based structure composed only of the antigen-recognizing part of the heavy and the light chain, i.e. a single-chain variable fragment (scFv). Alternatively, it is also possible to produce bispecific antibody-based constructs that are composed of two different antigen-recognizing parts derived from different antibodies.

## Blood-brain barrier

While for the most part organs tend to be highly accessible in the body for (radioactive) tracers that are injected into the bloodstream, the brain poses a challenge due to the blood-brain barrier (BBB). It forms a unique hurdle as it actively (and passively) regulates passage of molecules going into and out of the brain. The BBB consists of a layer of endothelial cells interconnected by tight junctions, and together they form the capillary walls. As a result, passive diffusion from the blood into the brain is strongly hindered. The endothelial layer is surrounded by astrocytic feet, astrocyte projections, which support and regulate the endothelial cells.

Unlike commonly assumed, small molecules are also affected by the BBB and cannot readily cross it. For example, a small molecule like histamine (100 Da) crosses the BBB to the extent of 2% reaching the brain [101]. Small molecules need to have favorable characteristics in order to cross the BBB, namely a molecular mass under 400- to 500- Da threshold, and high lipid solubility [101, 102]. For antibodies however, it is unlikely to ever develop an antibody-based construct that will be below 500 Da in size, and these rules

likely do not apply. Conventional IgG antibodies (>150 kDa) typically do not reach concentrations above 0.1% of injected dose in brain. However there are transport mechanisms in place at the BBB that can be taken advantage of.

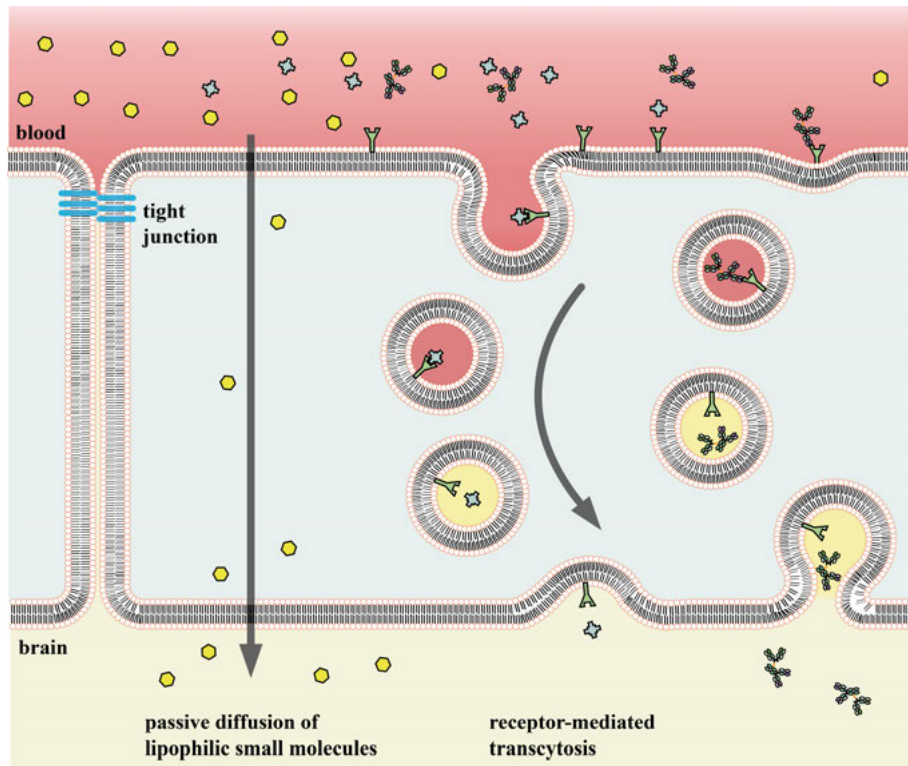


*Figure 3.* The blood-brain barrier is a selective barrier separating the brain from the rest of the body. It is composed of a layer of endothelial cells adjoined by tight junctions. Small molecules (e.g. water, and fat-soluble molecules) can diffuse across more easily than larger molecules. There is a myriad of receptor types present, facilitating transcytosis of essential nutrients and signaling molecules. One example of receptor-mediated transcytosis is the transferrin receptor (TfR), which is responsible for transporting iron molecules into the brain. When iron-bound transferrin binds to TfR, the process of transcytosis is initiated. Once the vesicle is fully formed, the pH drops from 7.4 (red vesicle) to 5.4 (yellow vesicle), causing the binding to the transferrin to dissipate, and the cargo is released into the brain side of the BBB. Similarly, this process can be utilized in order to transport TfR binding compounds such as a bispecific fusion protein recognizing TfR (right) across the BBB.

## Receptor Mediated Transcytosis

On the endothelial cell surface, there are many receptors present that induce endo- or transcytosis. The first evidence for an active receptor-mediated

transport (RMT) system came from the fact that insulin (5.8 kDa) can be found in the brain, but there is no insulin mRNA in the brain [103, 104]. As such, insulin in the brain must be from peripheral origin, and indeed human brain capillaries (i.e. the BBB) isolated from autopsied brains actively bind insulin with high affinity, indicating that there are mechanistic pathways present on the BBB for transporting larger molecules to the brain [105]. Similarly, another such example is the transferrin receptor (TfR) which is also found expressed on the BBB and is involved in iron transport into the brain. When transferrin forms a complex with iron, it will bind TfR and then enable RMT (**Figure 3**) [106]. The presence of endogenous RMT systems within the BBB enables a ‘Trojan Horse’ approach whereby a protein can cross the BBB via a receptor system (e.g. TfR) [107].

The first proof of concept of utilizing the transmembrane transport system to move a substance past the BBB was by Pardridge, when he demonstrated selective transport of an anti-TfR antibody through the BBB *in vivo* [108]. By coupling the anti-TfR IgG to another IgG with an intended intrabrain target, i.e. creating a bispecific fusion protein, it is then possible to transport your intended antibody into the brain. The affinity of the anti-TfR antibody is crucial here however, as a decreased affinity for TfR allows for release on the luminal side and thus increasing the transport into the brain [109].

High affinity binding to TfR caused a dose-dependent reduction of brain TfR levels, as rather than being released on the luminal side, the antibodies instead were trafficked to lysosomes as to be degraded. Moreover, an initial high affinity anti-TfR dosing induced reduction in brain TfR levels and led to decreased brain exposure to a second dose of low-affinity anti-TfR, likely by also degrading TfR which reduced potential recycling [110]. Another issue with high affinity binding is that it causes acute clinical symptoms and reticulocyte toxicity in mice, reducing the affinity however attenuated these side effects in a dose-dependent matter [111]. Furthermore, the bispecific antibody used in this study targeted  $\beta$ -secretase and showed efficacy as dosing with bispecific antibody led to a reduction in brain A $\beta$  [109]. More evidence that strong TfR binding leads to lysosomal degradation comes from Niewoehner and colleagues who demonstrate that monovalent binding rather than bivalent binding improves transport across the BBB. Here, a monovalent binder is found to cross the BBB better than a bivalent binder. The bivalent binding was internalized faster, though significantly more was associated with lysosomal markers, furthermore there was a reduced amount of TfR recycled to the cell surface [112].

Aside from avidity (i.e. total net binding strength), another factor that appears to play a role in proper TfR-based RMT is pH dependent binding. Antibodies with weakened binding in low pH environments (i.e. late endosome) transport better across than pH independent bindings *in vitro* [113]. As such, it would seem that there is a careful interplay of binding strength and pH dependence in trafficking anti-TfR antibodies across the BBB.

# Methodology

## Animal models

Transgenic mice are commonly used as animal models in research, and animal models are essential in investigating mechanisms of disease in order to relate the pathological processes to the human situation. The ability to create transgenic animals has paved a way for new possibilities of disease study. The transgenic ArcSwe mouse used here is a disease model of A $\beta$  pathology as a result of expressing human A $\beta$ PP with two mutations: the Arctic mutation (E693G) and the Swedish (KM670/671NL), which lead to a higher tendency to form A $\beta$  protofibrils and an increased production and secretion of A $\beta$  respectively [20–22, 114].

The ArcSwe mouse is a suitable model for investigating the effects of A $\beta$  oligomers and protofibrils. As a result of the mutations, ArcSwe mice overexpress A $\beta$ PP up to a threefold increase, and show intraneuronal A $\beta$  in the hippocampus which accumulates with age. Intraneuronal A $\beta$  immunoreactivity is already present in 1-month-old ArcSwe mice, and increases with age until it peaks at 6- to 8-month-old mice. Plaque formation is widespread and the first plaques are visible in 6-month-old ArcSwe mice [114]. As for soluble A $\beta$ , protofibril levels in ArcSwe mice are strongly elevated compared with non-transgenic mice, and increases with aging. ArcSwe mice already starting from the age between 4 and 8 months, which are in an early stage of pathology, have deficits in spatial learning and memory retention as assessed with the Morris water maze. These behavioral deficiencies correlate strongly with the levels of A $\beta$  protofibrils in these mice, but not with total A $\beta$  load, i.e. insoluble A $\beta$  plaque [48]. Altogether, it appears the ArcSwe mouse has amyloid pathology and behavioral deficits that is likely caused by soluble protofibrillar A $\beta$ . ArcSwe mice have SDS-insoluble plaque deposits, which resembles plaques found in human AD brain as they are also highly insoluble. This is unlike the plaques found in Swe mouse brain that are more diffuse and loose [115].

The second transgenic mouse model used here is the Swe model. It overexpresses A $\beta$ PP with the Swedish mutation (KM670/671NL), which is a double mutation directly adjacent to the  $\beta$ -secretase cleavage site in A $\beta$ PP. As a result, the Swedish mouse has increased production of A $\beta$ , while the A $\beta$ 40/42 ratio is unaffected. The onset of pathology is slower than in the ArcSwe mouse, the Swe mouse typically develops plaques by 11-13 months of age but develops more rapid afterwards [115]. Furthermore, Swe mice have an age-

related decline of spatial learning, working memory, and contextual fear conditioning by >12 months, although this is already impaired as early as 6 months of age [116, 117]. However this work was performed using a different Swe mouse model (the Tg2576 model), and as such is not entirely comparable.

The usage of animal models has led to a great deal of insight, however rather than an actual imitation of AD, models such as the ArcSwe mouse are reflective of just one aspect of pathology due to a mutation in a gene. They are representative of familial EOAD, and may not take into account the myriad of environmental or unknown factors that likely play a role in the majority of AD cases, which are late onset. Nonetheless, the ArcSwe mouse is representative of A $\beta$  disease, and is therefore suitable for investigating A $\beta$  pathology.

## In vivo imaging – positron emission tomography

Positron emission tomography (PET) is a nuclear imaging technique capable of visualizing structures and biological processes in the body. It is based on the injection of a radioactively labeled compound or molecule, which has a target that it will bind to or a biological function. The radioactive isotope enables detection of the radioligand (sometimes denoted as “tracer”, as it is given in trace amounts).

Commonly used clinical PET isotopes are carbon-11 and fluorine-18. As the isotope undergoes beta decay, it releases an antimatter particle, a positron, which annihilates when colliding with an electron. Upon occurrence of this event, two gamma photons are produced that travel in opposite directions (with an angle of 180°). When they reach a scintillator, it creates a signal that is detected by the photomultiplier tubes or silicon avalanche photodiodes that make up the detector ring of the PET scanner. The location of the decay event is dependent on being able to match the coincidence, and the assumption of the opposite directionalities that the photons travel. A strict timing window (on the nanosecond scale) is applied to properly assume coincidence.

Locations that show large amounts of annihilation, are places containing high concentrations of radioactive tracer. It is then assumed that the target of interest is located to the site where the tracer accumulates, such as visualization of high radioactivity in the brain (a highly metabolically active organ) with [<sup>18</sup>F]FDG. [<sup>18</sup>F]FDG is the most widely used PET tracer, and it is a fluorine-18 labeled glucose analogue. Its uptake is a marker of glucose uptake which is correlated with tissue metabolism, as any region with a higher metabolic rate would require more energy and thus more [<sup>18</sup>F]FDG signal is present.

A more novel class of PET tracers is the antibody-based radioligands. Currently fairly common in oncology, antibodies are suitable molecules to be adapted as radioligands as they are more specific than conventional small molecules.

## PET data analysis

The acquired data can either be displayed as a static image showing the localization of radioactivity, or computed to investigate dynamic changes in radioactivity over time. This is required in order to quantify tracer concentrations (i.e. receptor density) with pharmacokinetic modeling. In order to obtain (semi)quantitative measurements, the standardized uptake ratio (*SUV*) is often used. The *SUV* is the image derived radioactivity concentration ( $C_{img}$ ) corrected for the injected dose per bodyweight ( $ID/BW$ ) (Eq. 1). It is a convenient evaluation parameter that allows one to compare between subjects (e.g. comparing regional tracer uptake in different genotypes). It does not require dynamic scanning or blood sampling, making it a convenient measurement.

$$SUV = \frac{C_{img}}{ID/BW} \quad \text{Eq. 1}$$

As a (semi)quantitative measurement, the SUV ratio (SUVR) can be used to investigate regional differences in uptake. Here, the SUVR is used to investigate regional tracer uptake compared with a reference region, often the cerebellum, which should be largely void of specific tracer binding, providing an indication of specific binding (Eq. 2).

$$SUVR = \frac{SUV_{ROI}}{SUV_{ref}} \quad \text{Eq. 2}$$

It is also possible to pharmacokinetically simplify and describe the process of tracer transport and uptake. With kinetic modeling, the drug-organism interaction is simplified into compartments [118, 119]. A compartment is a physical space in which the tracer is considered to be distributed uniformly, e.g. tracer concentration in blood or plasma. The simplest compartmental model is the two-compartment model, or one-tissue compartmental model (1TCM). Here, the first compartment is the input function (i.e. measured plasma/blood curve). The second compartment is the tracer concentration in tissue. The interaction between the two is characterized by two rate constants ( $K_1$  and  $k_2$ ). As such for a known concentration in blood, assuming a state of equilibrium, the tracer concentration in tissue would be defined by the net flux between compartments.

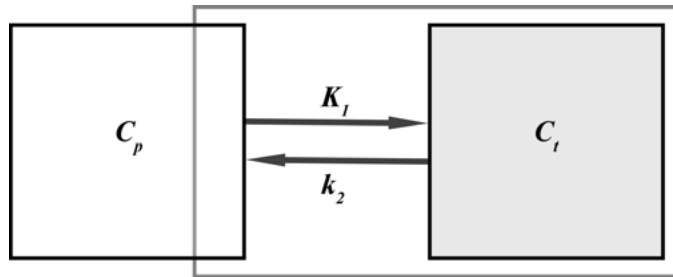


Figure 4. Schematic representation of a one-tissue compartmental model. It is the simplest model, and it requires arterial blood sampling. At equilibrium, tissue ( $C_t$ ) tracer concentrations are dependent on the blood concentration ( $C_p$ ). The flow from tissue back to the blood depends on the concentration in tissue.

It is sometimes possible to model receptor kinetics with a model without measuring the arterial input function, as to avoid performing arterial cannulation and metabolite measurements, if the reference model compares well to a model based on arterial blood sampling (i.e. the reference model must be validated). The simplified reference tissue model (SRTM) relies on the presence of a reference tissue region, void of specific binding of the ligand, and the assumption that the reference region and region of interest are identical otherwise, i.e.  $K_1/k_2 = K_1'/k_2'$  [120].

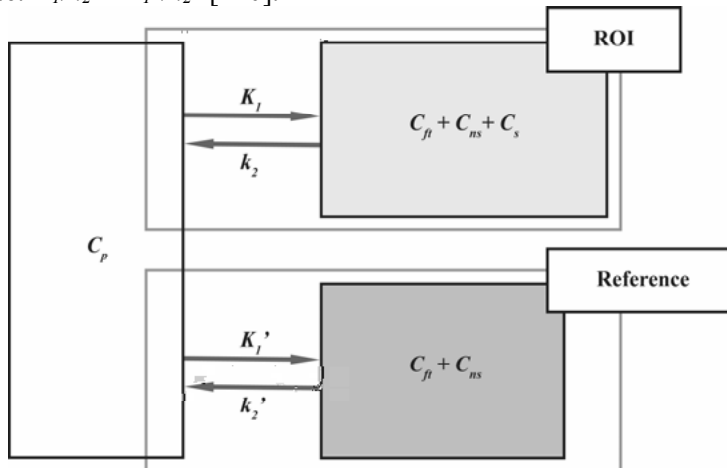


Figure 5. Schematic overview of the simplified tissue reference model. It is used for quantification of reversibly receptor binding tracers. No arterial blood sampling is required. Instead, it functions with the assumption that  $K_1/k_2 = K_1'/k_2'$ , and that the used reference region has negligible receptor density such that there is no specific binding. The cerebellum is an often used reference region for tracers such as [ $^{11}\text{C}$ ]ABP688, and [ $^{11}\text{C}$ ]raclopride, and also in this thesis for di-scFv [ $^{124}\text{I}$ ]3D6-8D3 and [ $^{124}\text{I}$ ]RmAb158-scFv8D3. The ROI is a target rich brain region of interest to be quantified.

Nondisplaceable binding potential ( $\text{BP}_{\text{nd}}$ ) is the sum of available receptor density and the affinity of the ligand to its target, and is the obtained measurement

from comparing the reference region to the receptor-rich region of interest. SRTM has been validated as a suitable method of reference tissue-based quantification of the metabotropic glutamate 5 receptor (mGluR5) [121]. Here, the calculated  $BP_{nd}$  obtained from calculating the equilibrium total distribution volume ( $V_T$ ) with a model requiring arterial sampling, and from SRTM in rats injected with [ $^{11}C$ ]ABP688, a selective tracer for mGluR5, found that reference tissue-based quantification proved to be suitable. The cerebellum was determined to be a valid reference region as it was largely empty of mGluR5, thus it has only negligible specific binding.

## Antibody conjugation

Prior to using recombinantly expressed fusion proteins, we used in **paper II** a chemically conjugated fusion protein composed of F(ab')<sub>2</sub>-h158 and 8D3. This was done by first modifying each antibody with one of two linkers which will bind specifically to each other to form a permanent bond. In order to purify, the mixed preparation was incubated with Fc-binding affinity matrix to specifically deplete unconjugated F(ab')<sub>2</sub> fragments. Then the mixture was incubated with IgGCH1 binding affinity matrix in order to deplete the sample of unconjugated 8D3. The purity of the preparation could then be assessed with on an unreduced SDS-PAGE stained with Coomassie Blue.

## Recombinant antibody expression

In order to produce recombinant bispecific constructs, first the sequences encoding the construct were cloned into a pcDNA3.4 vector. For di-scFv 3D6-8D3 (**Figure 6D**), this sequence was composed of the light and heavy chain variable fragments of scFv 3D6 linked together with a 15 amino acid sequence linker, followed by a 19 amino acid sequence linking the scFv 8D3 sequence, which was composed of the 8D3 heavy chain linked to the light chain with a 13 amino acid sequence. For purification purposes, a histidine-tag was attached on the C-terminus.

For RmAb158-scFv8D3 (**Figure 6C**), the sequence of scFv 8D3 was attached to the C-terminus of each RmAb158 light chain sequence via a short, inflexible peptide linker designed to hinder bivalent TfR binding. The heavy and the light chain are each on their own vector.

In order to obtain recombinant fusion protein, Expi293 cells were transfected with plasmid DNA encoding either di-scFv 3D6-8D3, or a 7:3 ratio mixture of light:heavy chain encoding RmAb158-scFv8D3. Following a 7-12 day incubation period post-transfection, the cell media was harvested and the antibody could be obtained via affinity purification. By running the cell media

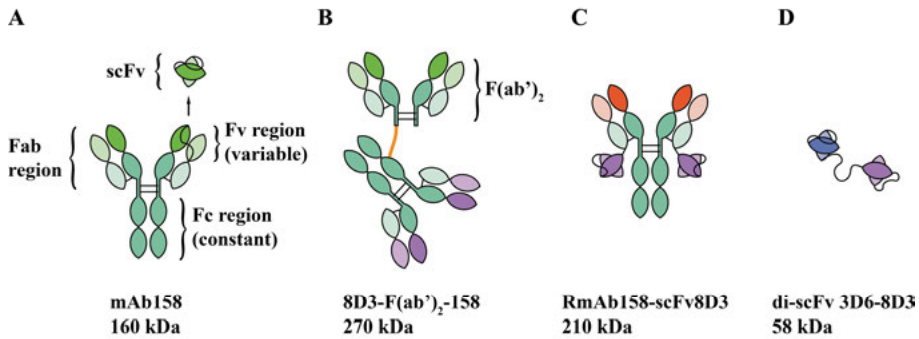


**Figure 6.** Schematic representation of conventional IgG (**a**), conjugated fusion protein (**b**), and two different formats of recombinant bispecific antibody-based constructs (**c-d**). The Fab region contains the variable region (Fv region) which is the antigen recognizing part of the IgG. Depicted here (**a**) is mAb158, a monoclonal mouse-derived IgG that recognizes the specific conformation of protofibrillar A $\beta$ . **b**. 8D3-F(ab')<sub>2</sub>-158 is a chemically conjugated bispecific fusion protein composed of IgG 8D3 (binds to mouse transferrin receptor (TfR)) linked to a F(ab')<sub>2</sub> fragment of mAb158 (i.e. the Fc region has been enzymatically removed). **c**. Recombinantly expressed bispecific antibody, RmAb158-scFv8D3, where the scFv8D3 has been expressed together with the light chain of RmAb158. Construct contains two scFv8D3s which are attached via short, inflexible linker peptide sequences. **d**. Di-scFv 3D6-8D3 is composed out of two scFvs: scFv 3D6 (binds to N-terminus of A $\beta$ ), and scFv 8D3 (binds to mouse TfR). These have been expressed in one sequence, and are linked together by a long, flexible peptide sequence.

through an affinity column, functionally formed antibody will bind to the column while the rest of the cell media will simply flow through. In case of di-scFv 3D6-8D3, the purification occurs using a nickel ion column which binds histidine-tagged proteins strongly. In order to then obtain the bound protein, a high concentration of imidazole is run through the column which weakens the histidine binding to the nickel column.

For RmAb158-scFv8D3, purification occurs using a protein G column which binds the Fc-region of the IgG. Here, elution can be performed using a pH lowering solution (i.e. 0.7% acetic acid solution) which weakens the aforementioned binding.

## *Ex vivo* studies

*Ex vivo* analyses were an integral part of the studies in this thesis. In order to assess the transport into the brain, animals were sacrificed at different time points post-injection, then perfused with 50 ml 0.9% NaCl over 2 min. The perfusion is an integral step to be able to accurately assess the brain uptake at early time points (e.g. 2 h), since initially the concentrations of radioligand in blood will be extremely high and make it impossible to accurately assess specific uptake in the brain compared with the high signal from blood. Animals

that were PET scanned (e.g. at 24 or 72 h) were also analyzed *ex vivo* to validate PET-derived findings.

Furthermore, organs were also harvested to investigate peripheral uptake. To investigate the blood pharmacokinetics, blood samples were taken periodically (frequently early post-injection) in order to assess the biological half-life in blood.

To validate the PET findings, sections were placed on a positron-sensitive phosphor screens. The screen is sensitive to the radioactivity in the section it is exposed to and an image develops visualizing the distribution and localization of the radioactivity in the section with greater resolution.

In order to detect both endothelial cells using immunohistochemistry, and the radiolabeled antibody, we performed nuclear track emulsion in **paper II**. After the section has been immunostained for endothelial cells, it is exposed to an emulsion which is sensitive to radioactivity. By then developing the section it is possible to visually detect both the radiolabeled antibody and the immunohistochemical staining.

## Iodine-124 and iodine-125 labeling

The antibody-based PET studies in **paper II** and **IV** were performed using iodine-124 ( $^{124}\text{I}$ ) labeled antibody. Iodine-124 is a proton-rich isotope with a radioactive half-life of 100.3 h (4.18 days). Its modes of decay are 74.4% electron capture and 25.6% positron emission. As such, it is a suitable isotope for relatively long term experiments involving PET. Antibody labeling with iodine-124 was performed by chloramine-T labeling, which is based on electrophilic attack of the phenolic ring of tyrosine residues by oxidized iodine [122]. The reaction is subsequently stopped after 120 s by addition of sodium metabisulfate in PBS, and iodine-124 labeled antibody was purified using NAP-5 size exclusion columns. Since the reaction could potentially occur at any tyrosine residue, the labeling can lead to a fairly heterogeneous mixture with some antibody molecules labeled more or less than others.

The other iodine isotope used in this thesis was iodine-125 ( $^{125}\text{I}$ ). Iodine-125 has a radioactive half-life of 1427.8 h (59.49 days), and it decays by electron capture to an excited state of tellurium-125, which immediately decays by gamma decay. Due to its long half-life, it is a preferred isotope for antibody-labeling for long term experiments. Here, it was primarily used for *ex vivo* pilot studies.

## Fluorine-18 labeling

In **paper V**, we performed fluorine-18 labeling of RmAb158-scFv8D3 and di-scFv 3D6-8D3. Here, the labeling was based on a ‘click’ conjugation reaction

between two different substrates: trans-cyclooctene (TCO) and tetrazine. First, antibody was modified with TCO, which reacts with primary amines to form a covalent bond. Then, by fluorine-18 labeling the tetrazine, it is possible to click the [<sup>18</sup>F]tetrazine with TCO-antibody, and thus indirectly labeling the antibody with fluorine-18 (**Figure 7**).

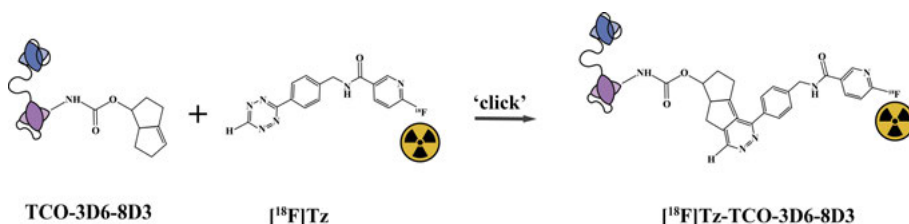


*Figure 7.* Scheme of TCO-Tetrazine ‘click’ reaction labeling. Antibody and TCO-tetrazine are not to scale.

## SDS-PAGE and immunoblotting

The process of separating macromolecules (i.e. proteins) using an electric field is called electrophoresis. Proteins are loaded into polyacrylamide gels (PAGE) which restrain larger molecules from migrating as fast as smaller molecules. Furthermore, the gel contains sodium dodecyl sulfate (SDS) which is an anionic detergent which in solution has a net negative charge. Proteins bind SDS proportionally to their relative molecular mass, and because of the negative charges they are strongly attracted towards a positively charged electrode (anode) in an electric field. As such, it is possible to separate proteins by molecular weight and to determine protein abundance and distribution. In order to visualize the proteins in the gel, they are stained with Coomassie Blue which is a dye that binds strongly to proteins.

After performing SDS-PAGE, the proteins can be transferred out of the gel into a nitrocellulose or polyvinylidene difluoride (PVDF) membrane. Again, an electric current is used to migrate the protein, in this case from the gel into the membrane while maintaining the distribution they had in the gel. It is then possible to visualize specific targets with antibodies, i.e. immunoblotting. By incubating the membrane with primary antibodies against the protein of interest, then with a subsequent incubation with a secondary antibody against the primary (the secondary is the detection antibody, linked to e.g. a fluorescent probe for detection), one can detect, visualize, and quantify the protein target of interest (**Figure 8A**). The advantage of this two-step process is signal amplification (i.e. several secondary antibodies can bind to the primary), and flexibility and cost-reduction. Generally, the secondary antibody is directed against a species-specific antigen, so that they can be used against varying primary antibodies of the same species.

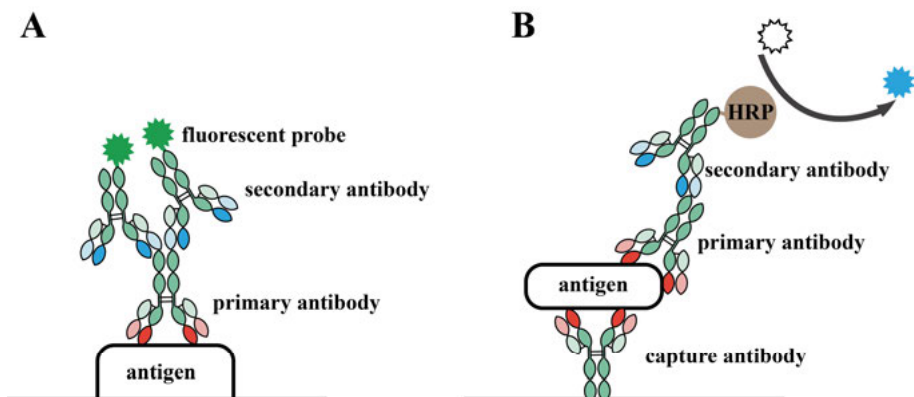


**Figure 8.** **A.** Schematic representation of two-step detection of a target of interest. First, the protein of interest (i.e. antigen) is bound by the primary antibody specifically recognizing its respective antigen. For detection and amplification, a secondary antibody specific for the primary antibody host species has a fluorescent probe, providing a detection readout. **B.** Sandwich ELISA layout. First, the antigen is captured by a capture antibody coated on the well surface, followed by binding by the primary antibody (often an antibody that binds to a different epitope of the same target), which is subsequently bound by the secondary antibody. The secondary antibody is generally biotinylated. Biotin binds to streptavidin, so by adding streptavidin-HRP, detection will be possible as HRP converts a substrate (TMB) into a detectable colored reaction product (blue).

## Immunofluorescence

Similarly to immunoblotting, immunofluorescence also relies on antibody binding to its antigen to detect and visualize the protein target of interest (**Figure 8A**). The main difference here is that immunofluorescence is performed on tissue sections in order to investigate the distribution of the protein in the native situation. First, the tissue is incubated with a primary antibody against the target of interest, then followed by an incubation with a detection secondary antibody directed against the species of the primary antibody. The signal can then be visualized under a fluorescence microscope.

## Cy3-labeling of antibodies

As another method for visualizing the antibody and its distribution, antibodies were labeled with a Cy3 fluorescent probe. The fluorescently labeled antibody was then intravenously injected into transgenic and wt mice, and brains were harvested 1 and 3 day post-injection and sectioned. As such, the immunostaining step occurred *in vivo*, followed by a histological readout.

## Enzyme linked immunosorbent assay

ELISA (enzyme linked immunosorbent assay) is an enzymatic reaction based diagnostic method for detection of an antigen of interest. Akin to immunoblotting and immunofluorescence, ELISA relies also on antibody binding to its antigen. The detection antibody has a horseradish peroxidase enzyme linked to it, which catalyzes the conversion of a substrate substance into a detectable form. Here, TMB (3,3',5,5'-Tetramethylbenzidine) was used which is converted into a blue color. Upon stopping the reaction with an acid or other stop reagent (i.e. sulfuric acid), TMB turns yellow and the readout is detectable color signal at 450 nm. Another difference is the way ELISAs are performed.

*Sandwich ELISA:* For detecting the presence and concentration of an antigen in a sample, sandwich ELISAs were performed (**Figure 8B**). First, the surface is coated with a capture antibody, which will bind the antigen present in the applied sample. A primary antibody recognizing the antigen is then added, and thus the antigen is 'sandwiched' between two antibodies. For detection, a secondary antibody bound to HRP is added which will enzymatically convert a substrate into a detectable reaction product. Alternatively, the secondary antibody can be biotinylated and then streptavidin-HRP is applied, which binds to biotin. Thus, the amount of enzymatic conversion is a readout of the antigen concentration.

*Competition ELISA:* For the purpose of measuring the antibody specificity to its antigen, competition ELISAs were performed. Here, the surface is instead coated with antigen, and a serial dilution of unlabeled competitor antibody mixed with biotinylated antibody is applied as sample. The signal can then be detected using streptavidin-HRP (which binds to biotin). Here, the signal intensity is inversely correlated to the concentration of unlabeled competitor antibody, i.e. more unlabeled antibody means less biotinylated antibody can bind and thus the signal intensity will be lower. With this method it is also possible to compare affinities of different antibodies to the same antigen, when the concentrations are equal, then the difference in signal intensity is a result of a difference in binding affinity.

*Inhibition ELISA:* In order to investigate the specific binding to different conformations of A $\beta$  (i.e. monomeric and protofibrillar forms), inhibition ELISAs were done. The surface is coated with A $\beta$  protofibrils, and a constant concentration of antibody preincubated with a serial dilution of A $\beta$  monomers or protofibrils was then loaded. The higher the affinity for the preincubated form of A $\beta$ , then less unbound antibody would be available for binding to the surface-coated A $\beta$  protofibrils, and thus the difference in signal readout is directly related to the antibody's conformational preference.

# Aim

The general aim of this thesis has been to discover/create a PET tracer capable of visualizing longitudinal and dynamic changes in the pathology related to AD.

In **paper I**, the approach taken was to investigate a key target which is considered to be functioning aberrantly due to a pathological interaction with A $\beta$  oligomers: the metabotropic glutamate receptor 5 (mGluR5). As such, the aim of **paper I** was to characterize the mGluR5 pathology on a protein level, and then to investigate whether it would be feasible as an *in vivo* PET biomarker for AD disease stage/severity.

In **paper II**, a different approach was taken instead. Here, we developed our own PET radioligand based on an antibody, with the rationale being that antibodies are more sensitive and can bind to a more specific epitope and/or conformation – providing a potential better readout than conventional small molecular radioligands. By doing so, we would be able to specifically target the soluble aggregated forms of A $\beta$  (protofibrils), and have a pathology-specific PET radioligand. The major issue with an antibody-based approach is the BBB. Conventional antibodies are unable to cross the BBB due to their size, as the BBB hinders passive diffusion. In order to get our antibody-based PET tracer into the brain, we chemically conjugated the A $\beta$  protofibril selective antibody (mAb158) to a TfR-specific antibody (8D3), thus creating a bispecific fusion protein. TfR is expressed on the surface of endothelial cells of the BBB and is involved in transporting transferrin across into the brain.

In **paper III**, we further improved and optimized our previously developed bispecific antibody format. Whereas in **paper II**, antibodies were chemically conjugated, which led to heterogeneous and impure preparations, we now designed and recombinantly expressed our bispecific antibodies – the methodology of which was published as **paper III**.

In **paper IV**, due to the findings of **paper III**, we were able to further improve our bispecific antibody-based approach. Rather than designing conventional antibodies, we instead utilized smaller formats that retain binding properties of the original antibody, but are instead a fraction of the size (i.e single-chain

variable fragments, or scFv), which are only 28 kDa whereas a conventional IgG antibody is 160 kDa.

In the final paper, **paper V**, a step is taken towards translation into the clinic. Previously, iodine-124 was utilized as the isotope to label our antibody-based PET ligands with. However, iodine-124 is an impure positron emitter (25.6%), furthermore it has a radioactive half-life of 4.18 days. As such, the focus of his paper was to perform fluorine-18 labeling of our antibody-based PET constructs. An issue in general with conventional antibodies is their long biological half-life in blood, which leads to poor signal-to-noise ratio. Previously, to circumvent this, we labeled with iodine-124 and waited at least 3 days before performing PET scans. However, in **paper IV**, we created a much smaller bispecific antibody construct, and we showed that it has a remarkably shorter biological half-life (3 h).

# Results

## Paper I

The disease-causing mechanisms leading to AD remain elusive. Soluble A $\beta$  oligomers are considered toxic, and their pathological role requires mediation via mGluR5. As such, the aim of the study is to investigate age and genotype related changes in mGluR5 in a mouse model of A $\beta$  pathology using PET with [ $^{11}\text{C}$ ]ABP688.

Wild type (wt) and transgenic ArcSwe mice, (at 4, 8, or 16 months of age) were used in this study. Mice were i.v. injected with [ $^{11}\text{C}$ ]ABP688, a highly selective noncompetitive antagonist for mGluR5, and scanned for 45 min to image mGluR5. After PET scanning, animals were transcardially perfused, and the level of radioactivity was measured in the extracted blood and brain tissue. The left hemisphere of the brain was then used to assess protofibril and mGluR5 levels, and the right hemisphere was used for immunofluorescence. Using SRTM with the cerebellum (known to have no mGluR5 expression) as reference region, we investigated the nondisplaceable binding potential in the following regions of interest (ROI): hippocampus, thalamus, striatum, and whole brain excluding the cerebellum [120, 121].

We found high uptake of [ $^{11}\text{C}$ ]ABP688 in hippocampus, thalamus, and striatum in both wt and transgenic mice, regions known to express high levels of mGluR5 compared with the rest of the brain. When given a large dose of cold unlabeled ABP688, the PET signal disappeared. Immunoblotting showed decreased mGluR5 levels in 16-month-old wt mice compared with their age-matched ArcSwe counterparts, which had elevated levels similar to younger ArcSwe mice. The ArcSwe mice had increased levels of protofibrils at 4 months, and levels continued to steadily increase with age. Wt mice had low levels regardless of age. Lastly, in the hippocampus we found that mGluR5 typically tended to colocalize with astrocytic marker glial fibrillary acidic protein (GFAP).

While we found signs of a pathology-related change in mGluR5 levels in ArcSwe mice using immunoblotting, [ $^{11}\text{C}$ ]ABP688 PET did not differentiate between ArcSwe and wt mice. Immunoblotting revealed elevated mGluR5 levels in ArcSwe mouse brain that did not decline with age, unlike wt mice that showed a significant age-dependent decrease at 16 months of age compared with ArcSwe mice. Both types of mice displayed higher BP<sub>nd</sub> and PET signal in hippocampus, thalamus, and striatum, coinciding with known

mGluR5 expression patterns. Evidently, the results from measuring protein levels using immunoblotting were not in unison with obtained PET data, based on the assumption that a change in mGluR5 receptor concentration (as assessed with immunoblotting) would reflect a change in the PET signal and  $BP_{nd}$ . This discrepancy could possibly be explained by several factors.

Firstly, the cerebellum may be less than ideal as a reference region as it may not be void of mGluR5 in mouse [123]. There is evidence for mGluR5 dysregulation in several disorders such as Fragile X syndrome (FXS) and autism [124, 125], and these affect the cerebellum [126–128]. In FMS, a trinucleotide repeat expansion in the 5'-UTR of *fmr-1* leads to loss of expression of fragile X mental retardation protein (FMRP) [129]. Similarly, FMRP has been found to regulate A $\beta$ PP mRNA translation through mGluR5 activation, and *fmr-1* KO mice have increased A $\beta$ 40 and A $\beta$ 42 levels; and an mGluR5-specific antagonist (2-methyl-6-(phenylethynyl)pyridine) was able to block this effect [130]. It is therefore possible that in A $\beta$ PP mouse models, there is a differential expression of mGluR5 present affecting also the cerebellum to a degree that the cerebellum may not be as suitable of a reference region as it is in wt cerebellum.

Secondly, due to the size of the mouse brain and the spatial resolution of PET, the signal-to-noise ratio (SNR) may be insufficient for observing any potential difference. This is mostly due to the partial volume effect whereby local maxima are underestimated due to a reduction in signal from the surrounding, smoothing values in the region. This is especially troublesome in mice, as the resolution of the  $\mu$ PET/CT (approx. 0.5-1 mm) is relatively large compared to the mouse brain, not to mention in any region of interest.

Nonetheless, this is the first *in vivo* study of mGluR5 in an AD mouse model with [ $^{11}$ C]ABP688. We found higher  $BP_{nd}$  in regions known for high mGluR5 expression than in the rest of the brain, although receptor densities were lower than earlier published in an [ $^{11}$ C]ABP688 validation study in rat brain. These findings could potentially be due to partial volume effects [121].

All in all, [ $^{11}$ C]ABP688 appears to be a good specific mGluR5 tracer. However, we conclude that currently quantifying mGluR5 with [ $^{11}$ C]ABP688 has proven to be unfeasible in mice, at least in the ArcSwe mouse model used here, although our data suggests an interaction between mGluR5 and A $\beta$ .

## Paper II

Here, we based our approach on previously performed work with our mAb158 antibody, which is selective for soluble protofibrils, as a high affinity detection agent for the toxic variants of A $\beta$  in the brain for measuring disease severity [131]. Previously, the viability of mAb158 (labeled with iodine-125) has been assessed, and there was a significant increase in brain concentrations of [ $^{125}$ I]mAb158 72 hours post-injection in ArcSwe mice compared with wt mice

[132]. The brain concentrations were, however, too low for it to be used as a PET tracer.

The brain endothelium which makes up the BBB expresses high concentrations of TfR, and an anti-TfR receptor antibody may function as a transport vector via receptor mediated transcytosis [106, 108]. Previously, brain uptake of an anti-TfR receptor antibody was strongly increased compared to a control IgG2a antibody [108], thus proving the principle of a molecular Trojan horse: creating a fusion protein where the therapeutic antibody or drug is linked to a second antibody that binds a specific receptor on the BBB, enabling receptor-mediated delivery of the fusion protein so it may reach its target in the brain [133].

Therefore, in order to increase uptake of our tracer into the brain, we created a fusion protein composed of a F(ab')<sub>2</sub> fragment of mAb158, recognizing the toxic soluble protofibrils, and a TfR antibody allowing the whole bispecific fusion protein to enter the brain sufficiently to enable PET imaging.

First, we enzymatically cleaved mAb158 to create a F(ab')<sub>2</sub> version of mAb158, which reduces its systemic half-life from 11 days to approximately 2 h in ArcSwe and wt mice. This increases the brain-to-blood ratio ( $K_p$ ), important for successful PET imaging, and decreases radiation dose for the patient. The F(ab')<sub>2</sub> fragment was then chemically conjugated to 8D3, an anti-TfR antibody, creating the 8D3- F(ab')<sub>2</sub>-mAb158 fusion protein (which had a half-life of about 15 hours). We radioiodinated 8D3-F(ab')<sub>2</sub>-mAb158 in order to perform *ex vivo* analyses. By labeling it with iodine-124, we created a PET tracer and injected ArcSwe, Swe, and wt mice with [<sup>124</sup>I]8D3-F(ab')<sub>2</sub>-mAb158. A 60 min PET scan was then performed 72 post injection. Animals were transcardially perfused with 0.9% NaCl, the left hemisphere was used for biochemical analysis, and the right for immunohistochemistry, autoradiography, and nuclear track emulsion autoradiography.

$K_p$  reached its maximum measured peak at 72 h post injection, although this could potentially have been higher if we had measured later as well. At this time point (72 h) ArcSwe mice had a significantly greater brain retention of 8D3-F(ab')<sub>2</sub>-mAb158 compared with F(ab')<sub>2</sub>-mAb158 (15-fold difference). Wt mice showed no significant uptake of 8D3-F(ab')<sub>2</sub>-mAb158, or F(ab')<sub>2</sub>-mAb158. When we performed PET at this time with [<sup>124</sup>I]8D3-F(ab')<sub>2</sub>-mAb158, there was observable PET signal in the brain of 12- and 18-month-old ArcSwe mice. In Swe mice there was no PET activity visible at 12 months, however the signal was greater in Swe mice at 18 months than in ArcSwe of the same age. This is likely due to the slower onset of disease in the Swe model, however pathology also progresses faster once present. The brain was void of activity in wt mice of all ages, and in ArcSwe mice at 4 and 8 months of age.

Nuclear track emulsion on sections immunostained for CD31, an endothelial marker, revealed little colocalization between CD31 and fusion protein.

There is visible accumulation of fusion protein surrounding amyloid plaques as visualized with Congo red.

PET-signals correlated with A $\beta$  protofibril load, but not with A $\beta$ 40 or A $\beta$ 42 load. There appears to be a PET detection limit of A $\beta$  protofibril load that is not yet reached in 4- and 8-month-old ArcSwe mice, and 12-month-old Swe mice. ArcSwe animals had significantly elevated levels of A $\beta$  protofibrils at 12 months of age which could be visualized with PET, while age-matched Swe mice showed no such increase and their A $\beta$  protofibril levels remained below the detection threshold.

We found an age dependent increase in PET activity in ArcSwe and Swe mice, i.e. as they age they accumulate A $\beta$  protofibrils. While ArcSwe had positive PET signal at 12 months already, Swe mice of the same age did not. This may be explained by the difference in disease progression between the two models, as ArcSwe mice have dense A $\beta$  plaque pathology comparable to those in the human AD brain. Plaques first appear at 6 months of age, and there is a near-linear increase of soluble A $\beta$  protofibrils with age. Swe mice on the other hand have more diffuse plaques with a later onset and more rapid increase in A $\beta$  pathology.

With [ $^{11}\text{C}$ ]PIB PET, young 8 and 12 month mice had similar [ $^{11}\text{C}$ ]PIB retention as wt mice. The 18 month old ArcSwe and Swe mice had some [ $^{11}\text{C}$ ]PIB retention, primarily in cortical regions, however SUVRs were lower than those obtained with [ $^{124}\text{I}$ ]8D3-F(ab') $_2$ -mAb158 PET.

All in all, our results suggest that we have successfully created a bispecific fusion protein capable of crossing the BBB and visualizing A $\beta$  load. Evidently, the Trojan horse based immunoPET may be successfully employed as a neuroimaging method, applicable also for other targets in the brain.

## Paper III

Here, we established a methodological protocol for producing recombinantly expressed multivalent antibodies using a mammalian expression system. Previous methods have been reported, but generally only for monovalent antibodies. Furthermore, we have also produced antibody-based constructs with this protocol, and it is the first describing the transfection of the mammalian Expi293 cell line with PEI.

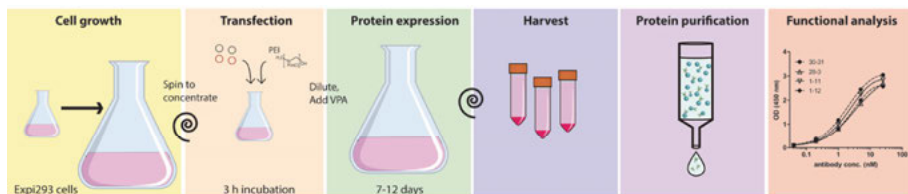


Figure 9. Scheme of recombinant protein expression pipeline.

Previously, Expifectamine™ has been the main reagent in use for transfecting Expi293 cells with the plasmid DNA encoding the protein-to-be-expressed. While it is an efficient reagent mixture, and very well suited for small batch transfection, its high cost (>1000-fold more expensive than PEI) makes it prohibitive for large scale transfection (i.e. > 100 ml media). Furthermore, here we used PEI 40K Max (Polysciences, Inc.), which is much easier to dissolve than the more conventionally used PEI 25K, further simplifying reagent preparation also.

All in all, establishing a lab protocol for recombinantly producing pure and homogeneous preparations of designed antibodies and antibody-based constructs has proven to be an important methodology underlying our current investigations.

## Paper IV

In **paper IV**, using the protocol previously described in **paper III**, we developed a small antibody-based bispecific construct named di-scFv 3D6-8D3 that is only 58 kDa (previous bispecific constructs were >200 kDa) which has a much reduced half-life in blood (3 h), whereas previous larger constructs were >11-16 h). The bispecific construct, di-scFv 3D6-8D3, is composed of two scFvs, 3D6 (3D6 is an N-terminal A $\beta$  binding antibody), and 8D3 (which binds to mouse TfR). Rather than using mAb158, 3D6 was chosen here as it binds monovalently to its target, while mAb158 requires bivalent binding (i.e. both arms of the IgG) since it is a conformation specific antibody. The scFv format of mAb158 has been explored, although here two scFv mAb158's were required for binding [134].

Owing to the much reduced half-life in blood, we were able to visually distinguish between transgenic mice and wild type already 1 day post-injection. Furthermore, this small construct has much higher SUVR (> 2–3) than PIB (conventionally >1.4 is considered PIB positive).

Another interesting finding is that this antibody, di-scFv 3D6-8D3, is based on an A $\beta$  N-terminal recognizing antibody (3D6), which does not have a preference for A $\beta$  conformation. Despite this, we found that our PET signal correlated best with levels of soluble A $\beta$  aggregates, and not with that of insoluble A $\beta$  plaques, despite there being 1000-fold more insoluble A $\beta$ . As such, it would appear that with regards to available binding sites (i.e. exposed N-terminals), soluble A $\beta$  is more easily accessible than insoluble A $\beta$ .

## Paper V

We were successful in fluorine-18 labeling RmAb158-scFv8D3 and di-scFv 3D6-8D3 using TCO-tetrazine click reaction. By first modifying the antibody

with TCO, it is receptive to being coupled to tetrazine. The tetrazine is the small molecule which prior to clicking will be fluorine-18 labeled, thus by clicking TCO-antibody to [<sup>18</sup>F]Tetrazine we will have created a fluorine-18 labeled antibody.

For validation purposes, we Cy3 labeled di-scFv 3D6-8D3 and injected it into ArcSwe and wt mice to visualize the antibody with a fluorescent approach. At 1 day post-injection there appeared to be a strong but diffuse signal present throughout the cortex of ArcSwe mice. Furthermore, surrounding plaques there was also a diffuse ‘halo’ of [Cy3]3D6-8D3, likely binding to any present soluble or available A $\beta$ . These patterns were also observed at 3 days post-injection but the signal intensity was weaker.

The BBB passage was investigated 2 h post-injection and we found [<sup>18</sup>F]RmAb158-scFv8D3 %SUV in brain of around 30%, and for di-scFv [<sup>18</sup>F]3D6-8D3 %SUV around 10% (in comparison, antibodies that would not be able to cross the BBB would not reach levels of >1%). As such, the antibody appeared to be functional after fluorine-18 labeling. Then, at 12 hours we investigated differences in retention in brain between wt and ArcSwe mice, and found a 2-fold difference between genotypes, which indicated that the antibody was being cleared in wt mice as they lack an intrabrain epitope for the antibody to bind to (i.e. no A $\beta$  pathology).

Initially with the first generation tetrazine (T1) we had significant uptake in skull and other bone tissue in a time dependent manner, indicating that this version defluorinated. However, the second (T2) and third (T3) generation tetrazines did not have this issue, as validated with PET.

Based on these encouraging findings, we decided to perform PET with di-scFv [<sup>18</sup>F]3D6-8D3 at 11-12 h post-injection, at which point only 1.55% of the initial injected activity remains (i.e. performing PET at a later time point would be challenging). The images obtained with T3-[<sup>18</sup>F]3D6-8D3 show higher uptake in ArcSwe mouse brain than in wt brain.

All in all, we appear to have successfully created and utilized a fluorine-18 version of an antibody-based PET tracer for visualizing A $\beta$  pathology in mouse brain.

# Reflections

The overall aim of this thesis has been to discover/create a PET tracer capable of visualizing longitudinal and dynamic changes in the pathology related to AD, and I believe that we have made some significant contributions.

Firstly, we have demonstrated the use of an antibody as a PET tracer for A $\beta$  pathology in the mouse brain. One of the most important aspects of this is that we have shown the possibility of selectively targeting a specific antigen and/or target, e.g. in this case the protofibrillar form of A $\beta$ . As such, this protofibril specific PET tracer can detect A $\beta$  pathology more accurately than conventional plaque imaging (i.e. [ $^{11}\text{C}$ ]PIB). This is further strengthened by the higher SUVR we have with antibody-based PET tracers compared with PIB, i.e. due to the specific binding to the soluble forms of A $\beta$ , which means that antibody-based PET appears to be more sensitive, which was also supported by the detection of pathology already at 8 months with antibody-based PET.

Furthermore, this thesis also serves as a proof-of-principle. PET tracers based on bispecific antibodies in general can also be adapted for other targets that underlie disease (e.g.  $\alpha$ -synuclein, or tau). One major advantage of antibody-based PET is the wide range of conventional antibodies already existing that can readily be adapted for use as a PET tracer. The specificity of antibodies means that it is possible to selectively target slight differences that could be the result of e.g. gene editing, familial mutations, polymorphisms (e.g. APOE isoform), or a specific (tau) isoform. This could lead to much improved detecting and diagnosing of disease.

While initially we used conventional antibodies that we then chemically conjugated in order to cross the BBB, later on we started expressing bispecific antibodies recombinantly which improved their purity and also function (as all recombinant antibodies were identical). Then, we started designing antibody-based constructs that were strongly reduced in size. The main rationale was that the size of the antibody directly correlated with the biological half-life in blood. By producing a 58 kDa di-scFv, we managed to reduce the biological half-life down to approximately 3 h, while previously a 210 kDa large bispecific antibody had a half-life of 11-16 h. In doing so, it was possible to detect and visually distinguish A $\beta$  pathology much earlier (1 day rather than 3 days post-injection). The shortened half-life can largely be explained also by the high concentrations of the 58 kDa construct found in urine and kidney (but

not for the 210 kDa antibody), which indicates that it is small enough to be cleared via the renal pathway. The rationale behind reducing the half-life is that for a PET tracer, the radioactive exposure should be as minimal as possible. In order to minimize, it is important also to shorten the biological half-life, as faster clearance would mean lower radioactive exposure. Furthermore, a shorter biological half-life also allows for earlier detection, and for using shorter-lived isotopes, e.g. fluorine-18.

As di-scFv 3D6-8D3 had the shortened biological half-life thus far developed in our hands, we attempted TCO-Tetrazine click chemistry in order to indirectly label it with fluorine-18. Click-chemistry also has other applications than fluorine-18 labeling. It can be a method to conjugate antibodies as well, in order to create bispecific antibodies that can then be tested *in vivo*, rather than expressing the entire bispecific construct which requires more than but also the entire known sequence for both antibodies. As such, click-chemistry allows for speedy creation of bispecific antibodies for other, new targets. As click-chemistry is possible *in vivo*, it can also be applied for pre-targeting. It is a different approach to cope with the pharmacokinetic limitations of conventional antibodies. First the TCO-modified antibody is administered and given time to clear peripherally. Then separately the radioactively labeled tetrazine is injected, and will click *in vivo* to the remaining antibody which should be specifically bound to its target. The tetrazine, being a smaller molecule, will then be eliminated quickly from blood. In doing so, it is possible to do PET with a large bispecific antibody and a short-lived isotope.

## Concluding remarks

Traditionally, small molecules have been the tracer type of choice for PET. These small and lipophilic compounds possess ideal properties for entering and reaching their intrabrain target. [<sup>11</sup>C]PIB was an imaging breakthrough for the AD field, as it is now an invaluable tool for detecting and diagnosing A $\beta$  plaque. However, the main downside to small molecules is their specificity (rather the rigidity thereof). Antibodies can potentially be used to target any thinkable antigen. Due to their immense size (approximately 400 times larger than small molecules), antibodies have difficulties crossing the BBB. By taking advantage of the endogenous transport mechanisms found on the BBB, it is possible to cross it using a Trojan horse, just as the ancient Greeks entered Troy. Once inside, the antibodies can bind and detect the specific target they were made to find. In this case, the soluble toxic forms of A $\beta$  (which PIB does not bind to).

The initial study (paper II) used a chemical conjugation method for making fusion proteins, leading to heterogeneous and suboptimally performing mixtures. By recombinantly designing and expressing the whole antibody-based construct as one protein, we obtained pure and better performing preparations.

Our initial fusion proteins were large molecules. As a result, their biological half-life in blood was long (>16 h). Reducing their size by using only one of the binding regions led to decreased half-lives, and made it possible to detect and distinguish a transgenic mouse from a wildtype at an earlier time point. The half-life of our (at this time) smallest construct (58 kDa) was short enough (3 h) that it was possible to use fluorine-18 (radioactive half-life: 1.83 h) as the labeling isotope, and to visualize differences already at 11 h post-injection.

Admittedly, the pharmacokinetic properties are still open to improvement. Ideally the biological half-life would be further reduced since at this point we still had to wait 11 hours before performing PET. However, at this point it is potentially not only the size of the antibody that is responsible for the half-life. Rather it appears that the transport via the transferrin receptor may have an influence on the pharmacokinetics.

Lastly, the TfR antibody (i.e. 8D3) used throughout this thesis is a mouse TfR binder. Thus, one of the major challenges for clinical adaptation of these antibodies in the near future will be to find or to create a suitable human TfR binder.

All in all, I believe that during the scope of this thesis, we made a significant contribution to the imaging field, and hope that we demonstrated the utility of antibodies as PET tracers.

# Acknowledgements

The work underlying this thesis was performed at the department of Public Health and Caring Sciences in the group of Molecular Geriatrics at the Rudbecklaboratory, Uppsala University. This work was made possible thanks to the financial support from the Swedish Research Council (#2012-1593), Alzheimerfonden, Hjärnfonden, Torsten Söderbergs stiftelse, Hedlunds stiftelse, Stiftelsen Fondkistan, Åhlén-stiftelse, Lindhés stiftelse, Stohnes stiftelse, Stiftelsen för Gamla tjänarinnor, Magnus Bergwalls stiftelse, and the Uppsala Berzelii Technology Centre for Neurodiagnostics.

First and foremost my supervisor, **Stina Syvänen**. I am deeply grateful for the opportunity to have worked here, and to have been able to learn so much about the PET imaging field. Sometimes I wonder, did you hire me because you previously spent time in the Netherlands...?

**Dag Sehlin**, my first co-supervisor and also the backbone of the group. I don't think I could have asked for a better mentor in all things Alzheimer's or wet lab related. Someday, I would like to try keeping a batch of your sourdough culture again.

And **Lars Lannfelt**, my last co-supervisor, for providing me with the opportunity to do my doctoral studies here.

I would also like to mention to my co-authors and collaborators, without whom very little would have probably been done. Most notably, **Jonas Eriksson**, our ever trusty radioactivity supplier. Someday, I hope I can get your business card.

My colleagues and the staff at the preclinical PET-MRI platform! Thank you **Sergio**, **Veronika**, **Ola** for all your help with anything ranging from practical matters to technical stuff. Special mention to **Ram**, if you weren't there to resuscitate the PET scanner all the time, I doubt we'd ever have published anything at all.

All current and previous members of **MolGer**, this lab would not have been the same without a single one of you. **Vilmantas**, **Ximena**, **Tobias**, **Martin**,

**Anna, Linn, Agata, Chiara, Ropa, Sahar, Sara, Jinar, Gabriel, Astrid, Greta, Sofia, Veronica, Linda, Therese, Elisabet I, Fadi, Aman, Xinge, Nami, Tor, Liza, and Malin.**

**Joakim**, the life of the lab. Atmospherically, working here would not have been the same without your passion for baseball, shoes, or cheetahs.

And all the guys and girls that I have spent way too much time drinking coffee with. Don't forget to invite me to your Indian wedding, **Anish**. **Maria**, yo sé que Suecia y Uppsala no son lo mismo que la ciudad de tu corazón, pero yo espero que tengas cuatro años felices. **Evangelos**, καλός άνθρωπος μου, I choose to believe that someday you will have your dream kitchen. **Silvio**, I have always wondered what life is like in the mountains. Turns out it's not too different from Swampy Germany, as we both share a funny pseudo-German sounding language and a love for cheese. **Elisabeth**, I hope the mousse recipe turns out as tasty as you remember it to be! Lastly, **Emma**, I look forward to the day you are getting a cat. **Robin** someday we will finish our D&D campaign.

My family for your support from abroad. Being abroad is not the easiest thing, but every time coming back, it felt like home.

**Leire**, where would I have been without you? I am lucky to have met you, and I am lucky to have you in my life. I look forward to our future adventures together.

## Summary

Alzheimer's disease is the most common form of dementia. It is a neurodegenerative disease. The first symptom is difficulty remembering recent events. As it worsens, symptoms can range from language problems, disorientation, mood swings, and behavioral issues. Clinical symptoms typically present around 70-80 years of age, although certain genetic forms present much earlier.

First reported by Alois Alzheimer in 1906 when he found protein deposits in the form of plaques and tangles in the brain of a 55 year old woman with what he called senile dementia. The plaques are largely made up of amyloid-beta ( $A\beta$ ), which in 1991 were proposed to be the cause of the disease.

At first, since the disease progress appeared to require mGluR5, which is a receptor protein involved in cell signaling. And so we decided to investigate if mice with AD-like pathology would have a different amount of mGluR5 as detected with a PET ligand (in this case, [ $^{11}C$ ]ABP688 is a PET tracer that binds to mGluR5). While we did find that these AD mice had more mGluR5 with *postmortem* investigations, using PET we could not detect these differences.

Then, our next approach was to try and target the actual disease causing forms of  $A\beta$ : the  $A\beta$  oligomers/protofibrils. These small, soluble forms of  $A\beta$  are considered the actual disease causing forms. The best way to do this was using an antibody. Antibodies are very specific, and can distinguish between an  $A\beta$  oligomer and the  $A\beta$  in the plaque. By doing so, the PET signal would indicate the amount of toxic  $A\beta$  in the brain. However, the issue is that antibodies are enormous molecules. For PET, conventional small molecules are 400 times smaller, and generally have no problems crossing the BBB.

The BBB is a layer of blood vessel-forming cells separating the brain from the rest of the body, and it prevents antibodies from entering. It selectively allows only certain kinds of molecules to cross into the brain, mainly nutrients and other molecules the brain needs. However, one particular molecule that does enter the brain is iron. Iron is actively transported by transferrin into the brain. Transferrin does this by binding to TfR on the BBB surface. By mimicking this binding to TfR with a TfR-binding antibody linked to the  $A\beta$  protofibril-recognizing antibody, we successfully transported antibodies into the brain, and we could detect the  $A\beta$  protofibrils with PET.

So the bispecific antibody created here was made using a chemical conjugation. This meant that the product was of a fairly mixed nature, as this chemical linkage could occur anywhere on either antibody.

Thus we established a method to design and express recombinant antibody-based constructs in mammalian cells, which gave us extremely pure and identical molecules. In doing so, we improved the reliability and sensitivity of our antibody-based PET tracers. It also allowed us to custom design the shape and size of our antibody-based molecules. Instead of having the entire antibody, we could use only the small part of it that binds to its target. As a result, our smaller bispecific antibody (58 kDa) was 4 times smaller than the previous recombinant bispecific antibody (210 kDa), and was eliminated from the body much faster. We could now already scan and detect A $\beta$  1 day after injecting, when before we had to wait at least 3 days.

In clinic, the most common radioactive isotope used is fluorine-18, which has a radioactive half-life of 109.8 minutes (every 109.8 minutes, half of the radioactivity decays, i.e. is gone). Previously, we used iodine-124 which has a half-life of 100.3 hours (aka 6018 min). So in order to minimize radioactive exposure and to make this antibody more suited for clinical use, we had to create a method for radioactively labeling it with fluorine-18 instead of iodine-124. We accomplished this using 'click' chemistry. Two molecules that bind together strongly when mixed: TCO and tetrazine. First, we linked TCO on our antibody. Then, we fluorine-18 labeled the tetrazine. Then, by mixing the TCO-labeled antibody with the fluorine-18 labeled tetrazine, we indirectly made a fluorine-18 labeled antibody. With this as a PET tracer, we successfully detected A $\beta$  already 11 hours after injection.

All in all, this thesis serves as a demonstration of using antibodies as PET tracers to detect the specific disease causing molecules and/or their specific shape (the oligomers/protofibrils). We have fine-tuned and improved the antibody-based tracer shape so that we could PET scan earlier. Antibody-based PET can of course also work for many other targets in the brain (such as the protein causing Parkinson's,  $\alpha$ -synuclein).

# Samenvatting

De ziekte van Alzheimer is de meest voorkomende vorm van dementie. Het is een neurodegeneratieve ziekte. Het eerste symptoom is moeite hebben met het herinneren van recente gebeurtenissen. Naarmate de ziekte erger wordt, presenteren zich meer symptomen zoals taalproblemen, disorientatie, stemmingswisselingen, en gedragsproblemen. Deze klinische symptomen beginnen typisch rond een jaar of 70-80, hoewel bepaalde genetische vormen al veel eerder beginnen.

De ziekte was voor het eerst gerapporteerd door Alois Alzheimer in 1906 toen hij eiwitten vondt in de vorm van *plaques* en *tangles* in het brein van een 55 jaar oude vrouw met wat hij seniele dementie noemde. Deze *plaques* bestaan voornamelijk uit het eiwit *amyloid-beta* ( $A\beta$ ), en in 1991 werd voorgesteld dat deze de oorzaak zijn van de ziekte.

Aanvankelijk begonnen wij ons onderzoek met het onderzoeken van *mGluR5* (metabotropic glutamate receptor 5), deze receptor is normaal betrokken met cellsignalering, en de functie van *mGluR5* was beschouwd als afwijkend in de ziekte van Alzheimer. Dus besloten we om te onderzoeken of transgene muizen met Alzheimer-pathologie een gewijzigde *mGluR5* concentratie hadden, en dit deden we d.m.v. [ $^{11}\text{C}$ ]ABP688 PET ([ $^{11}\text{C}$ ]ABP688 is een radioactieve molecuul die bind aan *mGluR5*). Hoewel we *postmortem* vonden dat deze Alzheimer muizen meer *mGluR5* eiwit hadden, konden we met PET geen verschillen zien.

Vervolgens besloten we ons te richten op de daadwerkelijke ziekte veroorzakende vorm van  $A\beta$ , namelijk de  $A\beta$  oligomeren en protofibrillen. Deze zijn kleine, oplosbare vormen van  $A\beta$  die nu beschouwd worden als daadwerkelijke boosdoeners. Om dit te doen, gebruikten we antilichamen. Antilichamen zijn ontzettend specifiek, en kunnen onderscheid maken tussen een  $A\beta$  oligomeer en de  $A\beta$  in de *plaques*. Dus als we een PET ligand gebaseerd op een antilichaam hadden, dan zou het PET signaal de hoeveelheid ziekteveroorzakende  $A\beta$  aantonen. Echter, het probleem nu is dat antilichamen enorme moleculen zijn. De gebruikelijke PET tracers (*small molecules*) zijn dan ook 400 maal kleiner dan antilichamen, en hebben ook over het algemeen geen probleem met het passeren van de bloed-hersenbarrière (BHB).

De BHB bestaat uit een laag cellen die de bloedvaten vormen, deze scheiden de hersenen af van de rest van het lichaam, en voorkomen dat grote moleculen zoals antilichamen de hersenen binnentreden. Het laatt alleen selectief bepaalde moleculen door, voornamelijk nutriënten en andere

voedingsstoffen die het brein nodig heeft. Eén zo'n stof is ijzer. Normaliter worden ijzer-moleculen actief de hersenen in getransporteerd door *transferrin*. *Transferrin* doet dit door zich te binden aan de *transferrin receptor (TfR)* op het oppervlak van de BHB. Door dit proces na te bootsen met een antilichaam, die zich ook aan de *TfR* bindt, welke gekoppeld is aan een  $A\beta$  protofibril-specifieke antilichaam, hebben wij onze bispecifieke antilichaam de hersenen in getransporteerd, en konden we de  $A\beta$  protofibrillen detecteren met PET.

De bispecifieke antilichaam was gecreëerd met een chemische conjugatie, wat betekent dat dit product een vrij heterogene preparatie is, omdat deze chemische koppeling specifiek overal kon plaatsvinden.

Daarom stelden wij een methode vast om recombinante bispecifieke constructen gebaseerd op antilichamen te ontwikkelen en te produceren in zoogdiercellen, welke tot extreme pure en identieke moleculen leidde. Zo verbeterden wij de betrouwbaarheid en gevoeligheid van onze op antilichaam-gebaseerde PET liganden. Verder was het nu ook mogelijk om de vorm en grootte van onze PET liganden aan te passen. In plaats van telkens de hele antilichaam te gebruiken, konden we alleen het kleine deel nemen dat daadwerkelijk binde. En zo creëerden wij een kleinere recombinante bispecifieke antilichaam (58 kDa) die 4 maal kleiner is dan onze vorige recombinante bispecifieke antilichamen (210 kDa), en deze was ook veel sneller geëlimineerd uit het lichaam. In plaats van 3 dagen te wachten, konden we nu al PET scannen en  $A\beta$  detecteren 1 dag na injectie.

In de kliniek is de meest gebruikte radioactieve isotoop fluor-18, die een radioactieve halveringstijd heeft van 109.8 minuten (e.g. iedere 109.8 minuten vervalt aka 'verdwijnt' de helft van de radioactiviteit). Eerder gebruikten wij jodium-124, welke een radioactieve halveringstijd heeft van 100.3 uur (6018 min). Om dus de radioactieve blootstelling te verkleinen en om deze antilichamen meer geschikt te maken voor gebruik in de kliniek, creëerden wij een methode om het te labelen met fluor-18 i.p.v. jodium-124. Dit was bereikt d.m.v. een scheikundige 'klik' reactie, twee moleculen die sterk met elkaar binden wanneer ze in dezelfde oplossing zijn: tetra cyclooctene (TCO) en tetrazine. Eerst bonden wij TCO aan een antilichaam, en labelden we de tetrazine met fluor-18. Door de TCO-antilichaam dan te mixen met fluor-18 gelabelde tetrazine, creëerden wij indirect een fluor-18 gelabelde antilichaam. Dit gebruikten we als de PET tracer en we waren in staat om  $A\beta$  11 uur na injectie al te visualiseren.

Al met al, deze thesis is een demonstratie van het gebruik van antilichamen als PET liganden om de specifieke ziekte veroorzakende moleculen en/of hun specifieke vorm dan wel conformatie te detecteren. Verder hebben we dit concept verfijnd en verbeterd om eerder en met betere gevoeligheid te kunnen PET scannen. PET liganden gebaseerd op antilichamen kunnen natuurlijk ook gemaakt worden voor vele andere doelen in het brein (bijv. het eiwit dat Parkinson's veroorzaakt,  $\alpha$ -synuclein).

# References

1. Klunk WE, Engler H, Nordberg A, et al (2004) Imaging brain amyloid in Alzheimer's disease with Pittsburgh Compound-B. *Ann Neurol* 55:306–19. doi: 10.1002/ana.20009
2. Mathis CA, Kuller LH, Klunk WE, et al (2013) In vivo assessment of amyloid- $\beta$  deposition in nondemented very elderly subjects. *Ann Neurol* 73:751–61. doi: 10.1002/ana.23797
3. Rodriguez-Vieitez E, Saint-Aubert L, Carter SF, et al (2016) Diverging longitudinal changes in astrogliosis and amyloid PET in autosomal dominant Alzheimer's disease. *Brain* 139:922–936. doi: 10.1093/brain/awv404
4. Engler H, Forsberg A, Almkvist O, et al (2006) Two-year follow-up of amyloid deposition in patients with Alzheimer's disease. *Brain* 129:2856–66. doi: 10.1093/brain/awl178
5. Aizenstein HJ, Nebes RD, Saxton JA, et al (2008) Frequent amyloid deposition without significant cognitive impairment among the elderly. *Arch Neurol* 65:1509–17. doi: 10.1001/archneur.65.11.1509
6. Okello A, Koivunen J, Edison P, et al (2009) Conversion of amyloid positive and negative mci to ad over 3 years: An c-pib pet study symbol. *Neurology* 73:754–760. doi: 10.1212/WNL.0b013e3181b23564
7. Maurer K, Volk S, Gerbaldo H (1997) Auguste D and Alzheimer's disease. *Lancet* 349:1546–1549. doi: 10.1016/S0140-6736(96)10203-8
8. Müller U, Winter P, Graeber MB (2013) A presenilin 1 mutation in the first case of Alzheimer's disease. *Lancet Neurol* 12:129–30. doi: 10.1016/S1474-4422(12)70307-1
9. Chow VW, Mattson MP, Wong PC, Gleichmann M (2010) An Overview of APP Processing Enzymes and Products. *NeuroMolecular Med* 12:1–12. doi: 10.1007/s12017-009-8104-z
10. Goldgaber D, Lerman MI, McBride OW, et al (1987) Characterization and chromosomal localization of a cDNA encoding brain amyloid of Alzheimer's disease. *Science* 235:877–80.
11. Palmert MR, Golde TE, Cohen ML, et al (1988) Amyloid protein precursor messenger RNAs: differential expression in Alzheimer's disease. *Science* 241:1080–4.
12. Matsui T, Ingelsson M, Fukumoto H, et al (2007) Expression of APP pathway mRNAs and proteins in Alzheimer's disease. *Brain Res* 1161:116–23. doi: 10.1016/j.brainres.2007.05.050
13. Bahmanyar S, Higgins GA, Goldgaber D, et al (1987) Localization of amyloid beta protein messenger RNA in brains from patients with Alzheimer's disease. *Science* 237:77–80.
14. Dahms SO, Hoefgen S, Roeser D, et al (2010) Structure and biochemical

- analysis of the heparin-induced E1 dimer of the amyloid precursor protein. *Proc Natl Acad Sci U S A* 107:5381–6. doi: 10.1073/pnas.0911326107
15. Xu H, Finkelstein DI, Adlard PA (2014) Interactions of metals and Apolipoprotein E in Alzheimer's disease. *Front Aging Neurosci* 6:121. doi: 10.3389/fnagi.2014.00121
  16. Tanzi RE, Bertram L (2005) Twenty years of the Alzheimer's disease amyloid hypothesis: A genetic perspective. *Cell* 120:545–555. doi: 10.1016/j.cell.2005.02.008
  17. Mann DMA, Esiri MM (1989) The pattern of acquisition of plaques and tangles in the brains of patients under 50 years of age with Down's syndrome. *J Neurol Sci* 89:169–179. doi: 10.1016/0022-510X(89)90019-1
  18. Glenner GG, Wong CW (1984) Alzheimer's disease and Down's syndrome: Sharing of a unique cerebrovascular amyloid fibril protein. *Biochem Biophys Res Commun* 122:1131–1135. doi: 10.1016/0006-291X(84)91209-9
  19. Waring SC, Rosenberg RN (2008) Genome-wide association studies in Alzheimer disease. *Arch Neurol* 65:329–34. doi: 10.1001/archneur.65.3.329
  20. Mullan M, Crawford F, Axelman K, et al (1992) A pathogenic mutation for probable Alzheimer's disease in the APP gene at the N-terminus of  $\beta$ -amyloid. *Nat Genet* 1:345–347. doi: 10.1038/ng0892-345
  21. Kamino K, Orr HT, Payami H, et al (1992) Linkage and mutational analysis of familial Alzheimer disease kindreds for the APP gene region. *Am J Hum Genet* 51:998–1014.
  22. Nilsberth C, Westlind-Danielsson A, Eckman CB, et al (2001) The "Arctic" APP mutation (E693G) causes Alzheimer's disease by enhanced A $\beta$  protofibril formation. *Nat Neurosci* 4:887–93. doi: 10.1038/nn0901-887
  23. Peacock ML, Warren JT, Roses AD, Fink JK (1993) Novel polymorphism in the A4 region of the amyloid precursor protein gene in a patient without Alzheimer's disease. *Neurology* 43:1254–6.
  24. Jonsson T, Atwal JK, Steinberg S, et al (2012) A mutation in APP protects against Alzheimer's disease and age-related cognitive decline. *Nature* 488:96–9. doi: 10.1038/nature11283
  25. Clark RF, Hutton M, Fuldner M, et al (1995) The structure of the presenilin 1 (S182) gene and identification of six novel mutations in early onset AD families. *Nat Genet* 11:219–22. doi: 10.1038/ng1095-219
  26. Borchelt DR, Thinakaran G, Eckman CB, et al (1996) Familial Alzheimer's disease-linked presenilin 1 variants elevate A $\beta$ 1-42/1-40 ratio in vitro and in vivo. *Neuron* 17:1005–13.
  27. Zhang Y, Thompson R, Zhang H, Xu H (2011) APP processing in Alzheimer's disease. *Mol Brain* 4:3. doi: 10.1186/1756-6606-4-3
  28. Ma H, Lesne S, Kotilinek L, et al (2007) Involvement of beta-site APP cleaving enzyme 1 (BACE1) in amyloid precursor protein-mediated enhancement of memory and activity-dependent synaptic plasticity. *Proc Natl Acad Sci* 104:8167–8172. doi: 10.1073/pnas.0609521104
  29. Kamenetz F, Tomita T, Hsieh H, et al (2003) APP Processing and Synaptic Function. *Neuron* 37:925–937. doi: 10.1016/S0896-6273(03)00124-7
  30. Haass C, Selkoe DJ (2007) Soluble protein oligomers in neurodegeneration: lessons from the Alzheimer's amyloid  $\beta$ -peptide. *Nat Rev Mol Cell Biol* 8:101–112. doi: 10.1038/nrm2101

31. Citron M, Diehl TS, Gordon G, et al (1996) Evidence that the 42- and 40-amino acid forms of amyloid  $\beta$  protein are generated from the  $\beta$ -amyloid precursor protein by different protease activities. *Proc Natl Acad Sci U S A* 93:13170–13175. doi: 10.1073/pnas.93.23.13170
32. Hardy J, Higgins G (1992) Alzheimer's disease: the amyloid cascade hypothesis. *Science* (80-) 256:184–185. doi: 10.1126/science.1566067
33. Karran E, Mercken M, Strooper B De (2011) The amyloid cascade hypothesis for Alzheimer's disease: an appraisal for the development of therapeutics. *Nat Rev Drug Discov* 10:698–712. doi: 10.1038/nrd3505
34. Terry RD, Masliah E, Salmon DP, et al (1991) Physical basis of cognitive alterations in Alzheimer's disease: synapse loss is the major correlate of cognitive impairment. *Ann Neurol* 30:572–80. doi: 10.1002/ana.410300410
35. Lue LF, Kuo YM, Roher AE, et al (1999) Soluble amyloid beta peptide concentration as a predictor of synaptic change in Alzheimer's disease. *Am J Pathol* 155:853–62.
36. McLean CA, Cherny RA, Fraser FW, et al (1999) Soluble pool of Abeta amyloid as a determinant of severity of neurodegeneration in Alzheimer's disease. *Ann Neurol* 46:860–6.
37. Walsh DM, Klyubin I, Fadeeva J V, et al (2002) Naturally secreted oligomers of amyloid beta protein potently inhibit hippocampal long-term potentiation in vivo. *Nature* 416:535–9. doi: 10.1038/416535a
38. Esparza TJ, Zhao H, Cirrito JR, et al (2013) Amyloid- $\beta$  oligomerization in Alzheimer dementia versus high-pathology controls. *Ann Neurol* 73:104–19. doi: 10.1002/ana.23748
39. Lesné S, Koh MT, Kotilinek L, et al (2006) A specific amyloid- $\beta$  protein assembly in the brain impairs memory. *Nature* 440:352–357. doi: 10.1038/nature04533
40. Gong Y, Chang L, Viola KL, et al (2003) Alzheimer's disease-affected brain: Presence of oligomeric A $\beta$  ligands (ADDLs) suggests a molecular basis for reversible memory loss. *Proc Natl Acad Sci* 100:10417–10422. doi: 10.1073/pnas.1834302100
41. Lambert MP, Barlow AK, Chromy BA, et al (1998) Diffusible, nonfibrillar ligands derived from Abeta1-42 are potent central nervous system neurotoxins. *Proc Natl Acad Sci U S A* 95:6448–53.
42. Hartley DM, Walsh DM, Ye CP, et al (1999) Protofibrillar intermediates of amyloid beta-protein induce acute electrophysiological changes and progressive neurotoxicity in cortical neurons. *J Neurosci* 19:8876–84.
43. Chimon S, Shaibat MA, Jones CR, et al (2007) Evidence of fibril-like  $\beta$ -sheet structures in a neurotoxic amyloid intermediate of Alzheimer's  $\beta$ -amyloid. *Nat Struct Mol Biol* 14:1157–1164. doi: 10.1038/nsmb1345
44. Noguchi A, Matsumura S, Dezawa M, et al (2009) Isolation and characterization of patient-derived, toxic, high mass Amyloid  $\beta$ -protein (A $\beta$ ) assembly from Alzheimer disease brains. *J Biol Chem* 284:32895–32905. doi: 10.1074/jbc.M109.000208
45. Upadhya AR, Lungrin I, Yamaguchi H, et al (2012) High-molecular weight A $\beta$  oligomers and protofibrils are the predominant A $\beta$  species in the native soluble protein fraction of the AD brain. *J Cell Mol Med* 16:287–295. doi: 10.1111/j.1582-4934.2011.01306.x
46. Figueiredo CP, Clarke JR, Ledo JH, et al (2013) Memantine Rescues

- Transient Cognitive Impairment Caused by High-Molecular-Weight A Oligomers But Not the Persistent Impairment Induced by Low-Molecular-Weight Oligomers. *J Neurosci* 33:9626–9634. doi: 10.1523/JNEUROSCI.0482-13.2013
47. Rijal Upadhaya A, Capetillo-Zarate E, Kosterin I, et al (2012) Dispersible amyloid  $\beta$ -protein oligomers, protofibrils, and fibrils represent diffusible but not soluble aggregates: their role in neurodegeneration in amyloid precursor protein (APP) transgenic mice. *Neurobiol Aging* 33:2641–60. doi: 10.1016/j.neurobiolaging.2011.12.032
  48. Lord A, Englund H, Söderberg L, et al (2009) Amyloid-beta protofibril levels correlate with spatial learning in Arctic Alzheimer's disease transgenic mice. *FEBS J* 276:995–1006. doi: 10.1111/j.1742-4658.2008.06836.x
  49. Wood JG, Mirra SS, Pollock NJ, Binder LI (1986) Neurofibrillary tangles of Alzheimer disease share antigenic determinants with the axonal microtubule-associated protein tau (tau). *Proc Natl Acad Sci U S A* 83:4040–3. doi: 10.1097/00002093-198701030-00021
  50. Neve RL, Harris P, Kosik KS, et al (1986) Identification of cDNA clones for the human microtubule-associated protein tau and chromosomal localization of the genes for tau and microtubule-associated protein 2. *Mol Brain Res* 1:271–280. doi: 10.1016/0169-328X(86)90033-1
  51. Goedert M, Spillantini MG, Jakes R, et al (1989) Multiple isoforms of human microtubule-associated protein tau: sequences and localization in neurofibrillary tangles of Alzheimer's disease. *Neuron* 3:519–526. doi: 10.1016/0896-6273(89)90210-9
  52. Shin RW, Iwaki T, Kitamoto T, Tateishi J (1991) Hydrated autoclave pretreatment enhances tau immunoreactivity in formalin-fixed normal and Alzheimer's disease brain tissues. *Lab Invest* 64:693–702.
  53. Harada A, Oguchi K, Okabe S, et al (1994) Altered microtubule organization in small-calibre axons of mice lacking tau protein. *Nature* 369:488–491. doi: 10.1038/369488a0
  54. Cleveland DW, Hwo SY, Kirschner MW (1977) Physical and chemical properties of purified tau factor and the role of tau in microtubule assembly. *J Mol Biol* 116:227–247. doi: 10.1016/0022-2836(77)90214-5
  55. Jeganathan S, Von Bergen M, Brütlich H, et al (2006) Global hairpin folding of tau in solution. *Biochemistry* 45:2283–2293. doi: 10.1021/bi0521543
  56. Schweers O, Schönbrunn-Hanebeck E, Marx A, Mandelkow E (1994) Structural studies of tau protein and Alzheimer paired helical filaments show no evidence for beta-structure. *J Biol Chem* 269:24290–7.
  57. Ayers JJ, Giasson BI, Borchelt DR (2017) Prion-like Spreading in Tauopathies. *Biol Psychiatry*. doi: 10.1016/j.biopsych.2017.04.003
  58. Friedhoff P, von Bergen M, Mandelkow E-M, et al (1998) A nucleated assembly mechanism of Alzheimer paired helical filaments. *Proc Natl Acad Sci* 95:15712–15717. doi: 10.1073/pnas.95.26.15712
  59. Guo JL, Lee VMY (2011) Seeding of normal tau by pathological tau conformers drives pathogenesis of Alzheimer-like tangles. *J Biol Chem* 286:15317–15331. doi: 10.1074/jbc.M110.209296
  60. Goedert M, Spillantini MG, Cairns NJ, Crowther RA (1992) Tau proteins of

- alzheimer paired helical filaments: Abnormal phosphorylation of all six brain isoforms. *Neuron* 8:159–168. doi: 10.1016/0896-6273(92)90117-V
61. Hanger DP, Betts JC, Loviny TL, et al (1998) New phosphorylation sites identified in hyperphosphorylated tau (paired helical filament-tau) from Alzheimer's disease brain using nanoelectrospray mass spectrometry. *J Neurochem* 71:2465–2476. doi: 10.1046/j.1471-4159.1998.71062465.x
  62. Bancher C, Grundke-Iqbal I, Iqbal K, et al (1991) Abnormal phosphorylation of tau precedes ubiquitination in neurofibrillary pathology of Alzheimer disease. *Brain Res* 539:11–18. doi: 10.1016/0006-8993(91)90681-K
  63. Seubert P, Vigo-Pelfrey C, Esch F, et al (1992) Isolation and quantification of soluble Alzheimer's  $\beta$ -peptide from biological fluids. *Nature* 359:325–327. doi: 10.1038/359325a0
  64. Vangool WA, Kuiper MA, Walstra G, et al (1995) Concentrations of amyloid beta protein in cerebrospinal fluid of patients with alzheimers disease. *Ann Neurol* 37:277–279.
  65. Motter R, C V-P, Kholodenko D, et al Reduction of beta-amyloid peptide42 in the cerebrospinal fluid of patients with Alzheimer's disease. *Ann Neurol* 38:643–648.
  66. Spies PE, Verbeek MM, van Groen T, Claassen JAHR (2012) Reviewing reasons for the decreased CSF Abeta42 concentration in Alzheimer disease. *Front Biosci (Landmark Ed)* 17:2024–2034. doi: 10.1093/infdis/jis904
  67. Strozzyk D, Blennow K, White LR, Launer LJ (2003) CSF A 42 levels correlate with amyloid-neuropathology in a population-based autopsy study. *Neurology* 60:652–656. doi: 10.1212/01.WNL.0000046581.81650.D0
  68. Mehta PD, Pirttilä T, Mehta SP, et al (2000) Plasma and cerebrospinal fluid levels of amyloid beta proteins 1-40 and 1-42 in Alzheimer disease. *Arch Neurol* 57:100–105. doi: 10.1001/archneur.57.1.100
  69. Kanai M, Matsubara E, Isoe K, et al (1998) Longitudinal study of cerebrospinal fluid levels of tau, A beta 1-40, and A beta 1-42(43) in Alzheimer's disease: A study in Japan. *Ann Neurol* 44:17–26. doi: 10.1002/ana.410440108
  70. Lewczuk P, Lelental N, Spitzer P, et al (2014) Amyloid- $\beta$  42/40 cerebrospinal fluid concentration ratio in the diagnostics of Alzheimer's disease: Validation of two novel assays. *J Alzheimer's Dis* 43:183–191. doi: 10.3233/JAD-140771
  71. Blennow K (2004) Cerebrospinal Fluid Protein Biomarkers for Alzheimer's Disease. *NeuroRX* 1:213–225. doi: <http://dx.doi.org/10.1602/neurorx.1.2.213>
  72. Hesse C, Rosengren L, Vanmechelen E, et al (2000) Cerebrospinal fluid markers for Alzheimer's disease evaluated after acute ischemic stroke. *J Alzheimers Dis* 2:199–206.
  73. Otto M, Wiltfang J, Tumani H, et al (1997) Elevated levels of tau-protein in cerebrospinal fluid of patients with Creutzfeldt-Jakob disease. *Neurosci Lett* 225:210–212. doi: 10.1016/S0304-3940(97)00215-2
  74. Hesse C, Rosengren L, Andreasen N, et al (2001) Transient increase in total tau but not phospho-tau in human cerebrospinal fluid after acute stroke. *Neurosci Lett* 297:187–190. doi: 10.1016/S0304-3940(00)01697-9
  75. Fodero-Tavoletti MT, Rowe CC, McLean CA, et al (2009) Characterization

- of PiB Binding to White Matter in Alzheimer Disease and Other Dementias. *J Nucl Med* 50:198–204. doi: 10.2967/jnumed.108.057984
76. Veronese M, Bodini B, García-Lorenzo D, et al (2015) Quantification of [(11)C]PIB PET for imaging myelin in the human brain: a test-retest reproducibility study in high-resolution research tomography. *J Cereb blood flow Metab* 35:1771–82. doi: 10.1038/jcbfm.2015.120
  77. Stankoff B, Freeman L, Aigrot MS, et al (2011) Imaging central nervous system myelin by positron emission tomography in multiple sclerosis using [methyl-11C]-2-(4-methylaminophenyl)-6-hydroxybenzothiazole. *Ann Neurol* 69:673–680. doi: 10.1002/ana.22320
  78. Matsubara K, Ibaraki M, Shimada H, et al (2016) Impact of spillover from white matter by partial volume effect on quantification of amyloid deposition with [11C]PiB PET. *Neuroimage* 143:316–324. doi: 10.1016/j.neuroimage.2017.04.042
  79. Lopresti BJ, Klunk WE, Mathis CA, et al (2005) Simplified quantification of Pittsburgh Compound B amyloid imaging PET studies: a comparative analysis. *J Nucl Med* 46:1959–1972. doi: 10.1093/ndt/46/12/1959 [pii]
  80. Jack CR, Knopman DS, Jagust WJ, et al (2010) Hypothetical model of dynamic biomarkers of the Alzheimer’s pathological cascade. *Lancet Neurol* 9:119–128. doi: 10.1016/S1474-4422(09)70299-6
  81. G. R, M. L, H. R, et al (2014) Diagnostic accuracy of amyloid and FDG PET in pathologically-confirmed dementia. *Neurology* 82:no pagination.
  82. Zhang S, Smailagic N, Hyde C, et al (2014) (11)C-PIB-PET for the early diagnosis of Alzheimer’s disease dementia and other dementias in people with mild cognitive impairment (MCI). *Cochrane database Syst Rev* 7:CD010386. doi: 10.1002/14651858.CD010386.pub2
  83. Um JW, Kaufman AC, Kostylev M, et al (2013) Metabotropic glutamate receptor 5 is a coreceptor for Alzheimer  $\beta$  oligomer bound to cellular prion protein. *Neuron* 79:887–902. doi: 10.1016/j.neuron.2013.06.036
  84. Renner M, Lacor PN, Velasco PT, et al (2010) Deleterious effects of amyloid beta oligomers acting as an extracellular scaffold for mGluR5. *Neuron* 66:739–54. doi: 10.1016/j.neuron.2010.04.029
  85. Bruno V, Ksiazek I, Battaglia G, et al (2000) Selective blockade of metabotropic glutamate receptor subtype 5 is neuroprotective. *Neuropharmacology* 39:2223–30.
  86. Hu N-W, Nicoll AJ, Zhang D, et al (2014) mGlu5 receptors and cellular prion protein mediate amyloid- $\beta$ -facilitated synaptic long-term depression in vivo. *Nat Commun*. doi: 10.1038/ncomms4374
  87. Hamilton A, Esseltine JL, DeVries RA, et al (2014) Metabotropic glutamate receptor 5 knockout reduces cognitive impairment and pathogenesis in a mouse model of Alzheimer’s disease. *Mol Brain* 7:40. doi: 10.1186/1756-6606-7-40
  88. Janus C, Pearson J, McLaurin J, et al (2000) A beta peptide immunization reduces behavioural impairment and plaques in a model of Alzheimer’s disease. *Nature* 408:979–982. doi: 10.1038/35050110
  89. Schenk D, Barbour R, Dunn W, et al (1999) Immunization with amyloid-beta attenuates Alzheimer-disease-like pathology in the PDAPP mouse. *Nature* 400:173–177. doi: 10.1038/22124
  90. Games D, Adams D, Alessandrini R, et al (1995) Alzheimer-type

- neuropathology in transgenic mice overexpressing V717F beta-amyloid precursor protein. *Nature* 373:523–7. doi: 10.1038/373523a0
91. Wisniewski T, Frangione B (2005) Immunological and anti-chaperone therapeutic approaches for Alzheimer disease. *Brain Pathol* 15:72–7.
  92. Bayer AJ, Bullock R, Jones RW, et al (2005) Evaluation of the safety and immunogenicity of synthetic A 42 (AN1792) in patients with AD. *Neurology* 64:94–101. doi: 10.1212/01.WNL.0000148604.77591.67
  93. Pride M, Seubert P, Grundman M, et al (2008) Progress in the Active Immunotherapeutic Approach to Alzheimer’s Disease: Clinical Investigations into AN1792-Associated Meningoencephalitis. *Neurodegener Dis* 5:194–196. doi: 10.1159/000113700
  94. Holmes C, Boche D, Wilkinson D, et al (2008) Long-term effects of A $\beta$ 42 immunisation in Alzheimer’s disease: follow-up of a randomised, placebo-controlled phase I trial. *Lancet* 372:216–223. doi: 10.1016/S0140-6736(08)61075-2
  95. Oddo S, Billings L, Kesslak JP, et al (2004) A $\beta$  immunotherapy leads to clearance of early, but not late, hyperphosphorylated tau aggregates via the proteasome. *Neuron* 43:321–332. doi: 10.1016/j.neuron.2004.07.003
  96. Bard F, Cannon C, Barbour R, et al (2000) Peripherally administered antibodies against amyloid beta-peptide enter the central nervous system and reduce pathology in a mouse model of Alzheimer disease. *Nat Med* 6:916–9. doi: 10.1038/78682
  97. DeMattos RB, Bales KR, Cummins DJ, et al (2001) Peripheral anti-A $\beta$  antibody alters CNS and plasma A clearance and decreases brain A burden in a mouse model of Alzheimer’s disease. *Proc Natl Acad Sci* 98:8850–8855. doi: 10.1073/pnas.151261398
  98. Blennow K, Zetterberg H (2013) The Application of Cerebrospinal Fluid Biomarkers in Early Diagnosis of Alzheimer Disease. *Med Clin North Am* 97:369–376. doi: 10.1016/j.mcna.2012.12.012
  99. Sevigny J, Chiao P, Bussière T, et al (2016) The antibody aducanumab reduces A $\beta$  plaques in Alzheimer’s disease. *Nature* 537:50–56. doi: 10.1038/nature19323
  100. Tucker S, Möller C, Tegerstedt K, et al (2015) The murine version of BAN2401 (mAb158) selectively reduces amyloid- $\beta$  protofibrils in brain and cerebrospinal fluid of tg-ArcSwe mice. *J Alzheimers Dis* 43:575–88. doi: 10.3233/JAD-140741
  101. Pardridge WM (2005) The blood-brain barrier: Bottleneck in brain drug development. *NeuroRX* 2:3–14. doi: 10.1602/neurorx.2.1.3
  102. Pardridge WM (2012) Drug transport across the blood-brain barrier. *J Cereb Blood Flow Metab* 32:1959–72. doi: 10.1038/jcbfm.2012.126
  103. Coker GT, Studelska D, Harmon S, et al (1990) Analysis of tyrosine hydroxylase and insulin transcripts in human neuroendocrine tissues. *Mol Brain Res* 8:93–98. doi: 10.1016/0169-328X(90)90052-F
  104. Kojima H, Fujimiya M, Matsumura K, et al (2004) Extrapneumatic insulin-producing cells in multiple organs in diabetes. *Proc Natl Acad Sci U S A* 101:2458–63. doi: 10.1073/pnas.0308690100
  105. Pardridge WM, Eisenberg J, Yang J (1985) Human blood-brain barrier insulin receptor. *J Neurochem* 44:1771–8.
  106. Pardridge WM, Eisenberg J, Yang J (1987) Human blood-brain barrier

- transferrin receptor. *Metabolism* 36:892–895. doi: 10.1016/0026-0495(87)90099-0
107. Pardridge WM, Boado RJ (2012) Reengineering biopharmaceuticals for targeted delivery across the blood-brain barrier. *Methods Enzymol* 503:269–292. doi: 10.1016/B978-0-12-396962-0.00011-2
  108. Pardridge WM, Buciak JL, Friden PM (1991) Selective transport of an anti-transferrin receptor antibody through the blood-brain barrier in vivo. *J Pharmacol Exp Ther* 259:66–70.
  109. Yu YJ, Zhang Y, Kenrick M, et al (2011) Boosting Brain Uptake of a Therapeutic Antibody by Reducing Its Affinity for a Transcytosis Target. *Sci Transl Med* 3:84ra44–84ra44. doi: 10.1126/scitranslmed.3002230
  110. Bien-Ly N, Yu YJ, Bumbaca D, et al (2014) Transferrin receptor (TfR) trafficking determines brain uptake of TfR antibody affinity variants. *J Exp Med* 211:233–244. doi: 10.1084/jem.20131660
  111. Couch J a, Yu YJ, Zhang Y, et al (2013) Addressing safety liabilities of TfR bispecific antibodies that cross the blood-brain barrier. *Sci Transl Med* 5:183ra57, 1-12. doi: 10.1126/scitranslmed.3005338
  112. Niewoehner J, Bohrmann B, Collin L, et al (2014) Increased Brain Penetration and Potency of a Therapeutic Antibody Using a Monovalent Molecular Shuttle. *Neuron* 81:49–60. doi: 10.1016/j.neuron.2013.10.061
  113. Paterson J, Webster CI (2016) Exploiting transferrin receptor for delivering drugs across the blood-brain barrier. *Drug Discov Today Technol* 20:49–52. doi: 10.1016/j.ddtec.2016.07.009
  114. Lord A, Kalimo H, Eckman C, et al (2006) The Arctic Alzheimer mutation facilitates early intraneuronal Abeta aggregation and senile plaque formation in transgenic mice. *Neurobiol Aging* 27:67–77. doi: 10.1016/j.neurobiolaging.2004.12.007
  115. Philipson O, Hammarström P, Nilsson KPR, et al (2009) A highly insoluble state of Abeta similar to that of Alzheimer’s disease brain is found in Arctic APP transgenic mice. *Neurobiol Aging* 30:1393–405. doi: 10.1016/j.neurobiolaging.2007.11.022
  116. Hsiao KK, Chapman PF, White GL, et al (1999) Impaired synaptic plasticity and learning in aged amyloid precursor protein transgenic mice. *Nat Neurosci* 2:271–276. doi: 10.1038/6374
  117. Hsiao K, Chapman P, Nilsen S, et al (1996) Correlative memory deficits, Abeta elevation, and amyloid plaques in transgenic mice. *Science* 274:99–102.
  118. Gunn RN, Gunn SR, Turkheimer FE, et al (2002) Positron emission tomography compartmental models: A basis pursuit strategy for kinetic modeling. *J Cereb Blood Flow Metab* 22:1425–1439. doi: 10.1097/00004647-200212000-00003
  119. Gunn RN, Gunn SR, Cunningham VJ (2001) Positron emission tomography compartmental models. *J Cereb blood flow Metab* 21:635–652. doi: 10.1097/00004647-200106000-00002
  120. Lammertsma AA, Hume SP (1996) Simplified reference tissue model for PET receptor studies. *Neuroimage* 4:153–8. doi: 10.1006/nimg.1996.0066
  121. Elmenhorst D, Minuzzi L, Aliaga A, et al (2010) In vivo and in vitro validation of reference tissue models for the mGluR(5) ligand [(11)C]ABP688. *J Cereb Blood Flow Metab* 30:1538–49. doi:

- 10.1038/jcbfm.2010.65
122. Greenwood FC, Hunter WM, Glover JS (1963) THE PREPARATION OF I-131-LABELLED HUMAN GROWTH HORMONE OF HIGH SPECIFIC RADIOACTIVITY. *Biochem J* 89:114–23.
  123. Kubera C, Hernandez AL, Heng V, Bordey A (2012) Transient mGlu5R inhibition enhances the survival of granule cell precursors in the neonatal cerebellum. *Neuroscience* 219:271–9. doi: 10.1016/j.neuroscience.2012.05.064
  124. Dölen G, Bear MF (2008) Role for metabotropic glutamate receptor 5 (mGluR5) in the pathogenesis of fragile X syndrome. *J Physiol* 586:1503–8. doi: 10.1113/jphysiol.2008.150722
  125. Carlson GC (2012) Glutamate receptor dysfunction and drug targets across models of autism spectrum disorders. *Pharmacol Biochem Behav* 100:850–4. doi: 10.1016/j.pbb.2011.02.003
  126. Koekkoek SKE, Yamaguchi K, Milojkovic BA, et al (2005) Deletion of FMR1 in Purkinje cells enhances parallel fiber LTD, enlarges spines, and attenuates cerebellar eyelid conditioning in Fragile X syndrome. *Neuron* 47:339–52. doi: 10.1016/j.neuron.2005.07.005
  127. Huber KM (2006) The fragile X-cerebellum connection. *Trends Neurosci* 29:183–5. doi: 10.1016/j.tins.2006.02.001
  128. Casanova MF (2007) The neuropathology of autism. *Brain Pathol* 17:422–33. doi: 10.1111/j.1750-3639.2007.00100.x
  129. Oberle I, Rousseau F, Heitz D, et al (1991) Instability of a 550-base pair DNA segment and abnormal methylation in fragile X syndrome. *Science* (80- ) 252:1097–1102. doi: 10.1126/science.252.5009.1097
  130. Westmark CJ, Malter JS (2007) FMRP mediates mGluR5-dependent translation of amyloid precursor protein. *PLoS Biol* 5:e52. doi: 10.1371/journal.pbio.0050052
  131. Englund H, Sehlin D, Johansson A-S, et al (2007) Sensitive ELISA detection of amyloid-beta protofibrils in biological samples. *J Neurochem* 103:334–45. doi: 10.1111/j.1471-4159.2007.04759.x
  132. Magnusson K, Sehlin D, Syvänen S, et al (2013) Specific uptake of an amyloid- $\beta$  protofibril-binding antibody-tracer in A $\beta$ PP transgenic mouse brain. *J Alzheimers Dis* 37:29–40. doi: 10.3233/JAD-130029
  133. Pardridge W (2006) Molecular Trojan horses for blood–brain barrier drug delivery. *Curr Opin Pharmacol* 6:494–500. doi: 10.1016/j.coph.2006.06.001
  134. Syvänen S, Fang XT, Hultqvist G, et al (2017) A bispecific Tribody PET radioligand for visualization of amyloid-beta protofibrils – a new concept for neuroimaging. *Neuroimage* 148:55–63. doi: 10.1016/j.neuroimage.2017.01.004

# Acta Universitatis Upsaliensis

*Digital Comprehensive Summaries of Uppsala Dissertations  
from the Faculty of Medicine 1395*

Editor: The Dean of the Faculty of Medicine

A doctoral dissertation from the Faculty of Medicine, Uppsala University, is usually a summary of a number of papers. A few copies of the complete dissertation are kept at major Swedish research libraries, while the summary alone is distributed internationally through the series Digital Comprehensive Summaries of Uppsala Dissertations from the Faculty of Medicine. (Prior to January, 2005, the series was published under the title "Comprehensive Summaries of Uppsala Dissertations from the Faculty of Medicine".)

Distribution: [publications.uu.se](http://publications.uu.se)  
urn:nbn:se:uu:diva-333220



ACTA  
UNIVERSITATIS  
UPSALIENSIS  
UPPSALA  
2017